Exergy Assessment of Single and Dual Pressure Industrial Ammonia Synthesis Units

Daniel Flórez-Orrego [a], Silvio de Oliveira Junior [b]

Department of Mechanical Engineering, Polytechnic School, University of Sao Paulo, Sao Paulo, 05508-900, Brazil.
[a]daflorezo@usp.br ***CA****, [b]soj@usp.br*

Abstract:

In exothermic, equilibrium-limited processes such as ammonia synthesis, higher per-pass conversions are often achieved by withdrawing the enthalpy of reaction before the conversion has been completed. However, although inter-bed cooling may help controlling the bed feed temperatures and generates high pressure steam, it also shifts the reacting mixture away from equilibrium (i.e. by increasing the reacting driving force, $-\Delta G$), thus increasing the process irreversibilities. In order to offset the unfavorable effects of the bed intercooling in the decreasing-volume reactive system as well as to reduce the power consumption, a catalytic once-through conversion section is introduced in a 1000 metric t_{NH3}/day ammonia synthesis unit. Three unit configurations are analyzed: two are based on single pressure loops (SP150, SP200), whereas the other (DP) operates at two incremental levels of pressure (83/200bar). The dual pressure process aims to show the relevance of the Counteraction Principle for driving the system irreversibilities down. The plant-wide and main components' performance are also compared in terms of exergy efficiency, economic revenues and utilities consumption. As a result, the syngas compressor, ammonia converter, waste heat recovery and ammonia refrigeration systems are found to be responsible for about 80-86% of total irreversibilities in the ammonia loop, which varies from 23.8MW for DP and 27.2MW for SP150. A cryogenic purge gas treatment unit allows improving the loop performance in 9-13% if compared to non-hydrogen-recovery systems.

Keywords:

Ammonia, Dual Pressure, Exergy Destruction, Counteraction

1. Introduction

Currently, nearly 116.5 million of tons (as N) of nitrogen fertilizers are annually produced and the world demand is expected to increase more than 2.9 million of metric tons between 2016 and 2018 [1]. Fertilizers represent the second largest share in energy consumption (24%) in agriculture, only surpassed by fuels and followed far by pesticides (1.6%) [2]. They also account for about 2% of the total world energy consumption [3]. Ammonia is the basic feedstock for all upgraded nitrogen fertilizers and other industrial products. More than 80% of produced ammonia is used as agricultural fertilizer for food production, supplying 50 percent of all protein consumed by humans [4]. In Brazil, even though total installed capacity attains 1.5 million tons of ammonia per year, more than 60% of the domestic demand must still be imported [5]. This explains the fact that fertilizer industry has been the segment that contributed the most (25%) towards the total deficit in the Brazilian chemical sector [6]. Petrobras is currently performing an ambitious expansion plan to project and build new fertilizer plants, expecting all these projects to supply about 87% of the national ammonia demand by 2020 [7, 8]. Since more than 45% of the world ammonia plants are older than 30 years [9], major opportunities for revamps, even in plants already modified, are foreseeable. In fact, notwithstanding the level of energy integration and recent developments in modern ammonia plants, the specific exergy consumption has not been reduced radically so far. For instance, it is noteworthy that the minimum theoretical exergy consumption in ammonia plants is still much lower (18-21GJ/t_{NH3}) [9] than the best

figures reported in the literature (28-31 GJ/t_{NH3}), which vary widely with local conditions and project-specific requirements [10, 11]. According to The European Roadmap of Process Intensification (PI - PETCHEM), the potential benefits in the ammonia production sector are significant: 5% higher overall energy efficiency for the short/midterm (10-20 years) and 20% higher (30-40 years) for the long term [12]. The efforts have mainly focused on reducing power and feedstock consumption [11], improving the heat recovery network [13-19], minimizing stack losses, cutting energy consumption for CO_2 removal [20-22] and designing better and more active catalysts (Ru-based) [11, 23-26]. Recently, promoted ruthenium catalyst was introduced in commercial operation; however, it is not clear whether the improved activity of such catalysts is justified by the significantly higher cost and shorter life-time relative to the traditional iron catalyst [27, 28]. Other studies [29, 30] propose the implementation of an ammonia gas turbine to directly produce shaft work from the reactor effluent, as an alternative for steam generation. From an exergy point of view, this is a more efficient way of profiting the thermal and mechanical exergy for power production, as long as the number of operations involved is also reduced. According to [29], about 4 MW of electricity and 7350 kW of HP steam can be produced, whereas the total amount of exergy loss is reduced by 19% compared to the conventional process.

However, in the case when both conversion rate and loop capacity come up against their practical limits, the remaining possibility is to produce additional ammonia outside the actual synthesis loop, i.e. partially converting the fresh synthesis gas outside the loop [31, 32]. The installation of two synthesis loop in series or a pre-converter – i.e. a once-through synthesis converter in the makeup gas stream – has been previously studied in order to improve the conversion and keep the synthesis catalyst from poisoning [33]. However, since both sequential conversion sections have been operated at the same pressure, the potential benefits of gradually increasing the process pressure in the reduction of the exergy losses could not be highlighted. In the Uhde dual pressure process, the total ammonia production is split into an upstream low pressure, once-through conversion process and a conventional synthesis loop at high pressure with a reduced size [31, 32]. Dual pressure systems have been conceived to take advance of bigger plants by means of the economy of scale, as doubling the size of a single train plant has the potential to reduce the capital-related cost of production in about 20% [34]. Another way of using feedstock more efficiently, even at higher capital cost, consists of the recovery of hydrogen and ammonia from the purge gas by a cryogenic unit, which may result in an ammonia capacity increase of 5% (or the equivalent of feedstock economy) [34, 35]. Withal, exergy saving steps without an alternative use for saved exergy does not represent an economic criteria for making large capital investments, since improvement modifications are not always economical and even may adversely affect reliability [36]. Accordingly, caution is required when weighing a decision on the potential exergy savings against potential economic and environmental gains. Anyhow, the increasing of processes efficiency could be the first step towards the reduction of the large non-renewable exergy consumption and environmental impact that ammonia is responsible for. Thus, in this work, exergy is used to quantify the efficiency and compare the exergy destruction rates along the various components of the ammonia synthesis loop, while looking after attractive economic revenues as a function of the most critical operation parameters. It will be shown that the optimal design is rather a complex function of the standalone equipment performance and the interaction of all the synthesis loop components, even if largely influenced by the reactor performance.

2. Single and dual pressure ammonia synthesis unit description.

Figures 1 and 2 show the ammonia synthesis unit configurations studied, which typically include a syngas compression train, an ammonia reactor, a waste heat recovery network, a condensation and

refrigeration system and a purge gas treatment unit. These elements are strongly interrelated to each other's operating conditions, affecting simultaneously different sections of the loop concept. It is noteworthy that the cooling water heat exchangers are represented here as three-way devices, differently from actual four-way physical configurations. In the first configuration (Fig. 1), the ammonia synthesis is entirely achieved in a single pressure loop, where the unconverted gas is recycled to a reactor consisting of three catalytic beds. In the dual pressure unit depicted in Figure 2, the ammonia production occurs in two sequential conversion sections at different pressures. In the first section, the fresh syngas is compressed to about 83 bar in a multiple-stage intercooled compressor. Next, the syngas is fed to a multiple-bed once-through reactor where about 18% of the ammonia is produced. Next, about 60% of the ammonia is condensed and separated from the gas, and the remaining syngas is further compressed to 200 bar and fed to the high pressure synthesis loop [34]. One benefit of the early removal of ammonia is that, after the first ammonia conversion stage, the volume of the gas is reduced and, consequently, the amount of recirculated gas is also reduced. Besides, as it will be discussed later, by gradually increasing the pressure of a decreasing-volume reaction, the synthesis of ammonia can be performed in a more efficient way [37].

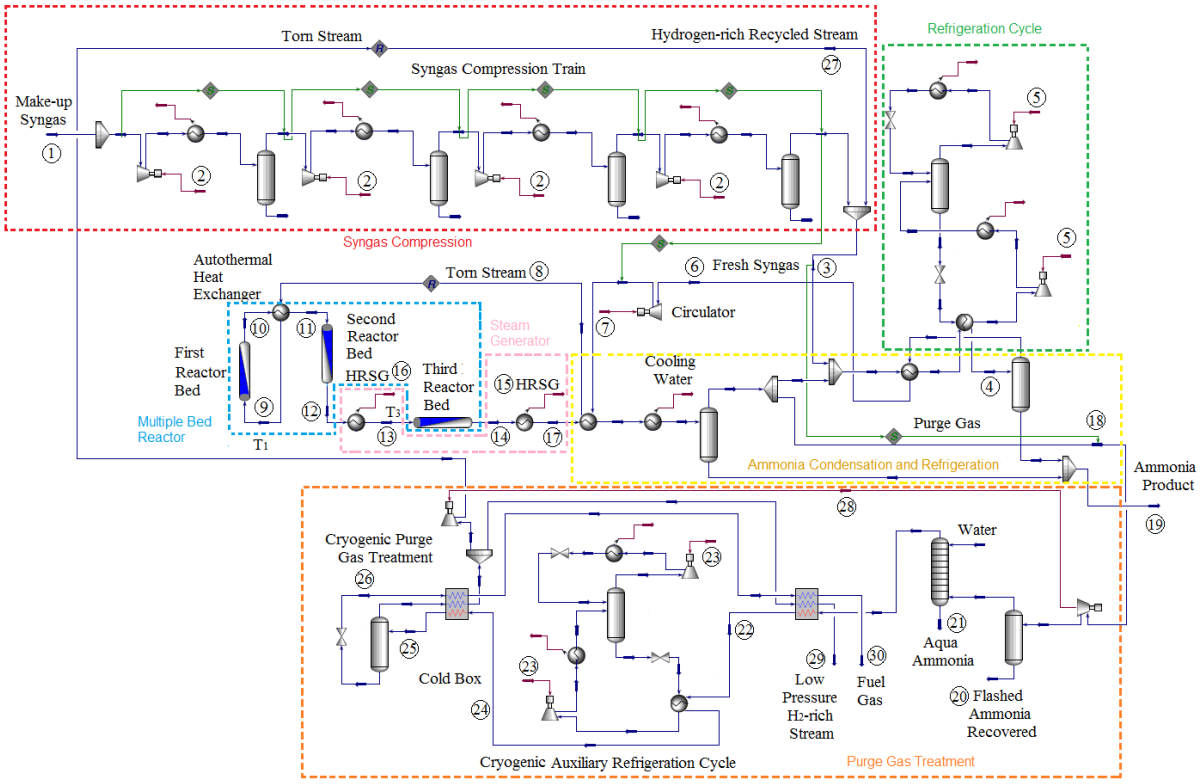

Fig. 1. Single Pressure Ammonia Synthesis flowsheet (see also Table A.1 and A.2).

The converter size and loop efficiency are affected by the reactor pressure, the feed temperature and composition, as well as by the amount of inerts and recycled ammonia, inter-bed cooling design and the catalyst used [3]. Typical degree of conversions between 10 to 20% are achieved in presence of an iron based catalyst [34]. Moreover, since ammonia condensation is not completely satisfactory if only water or air cooling is performed [38], the reactor effluent must be refrigerated to approx. -20°C via a double-stage R717 vapor compression system [3]. The build-up of inerts (argon, methane) in the loop must be also controlled by a continuous withdrawal of a portion of the hydrogen-rich recycle gas to keep their concentrations down to acceptable levels [35]. In older ammonia plants, the purge gas was

used as supplemental fuel for the primary reformer [39]. However, since its valuable hydrogen content represents readily available feedstock for ammonia synthesis, and in view of the considerable amount of energy that has been consumed in producing and compressing it to the loop pressure, hydrogen is preferably recovered and recycled to the synthesis loop [40]. Recovery processes may include cryogenic partial condensation, pressure swing adsorption (PSA) and membrane permeation [25]. For low-boiling compounds, cryogenics can achieve higher hydrogen recovery efficiencies (99.5%), while operating at high pressures and large molar flow rates [41]. On the other hand, PSA (20-30 bar) presents lower recovery efficiencies (70-85%) [25, 41] and membrane systems entails a considerable pressure drop [42, 43]. More capital intensive methods consider feeding the purge gas to a downstream synthesis loop operating at slightly lower pressure [9, 44].

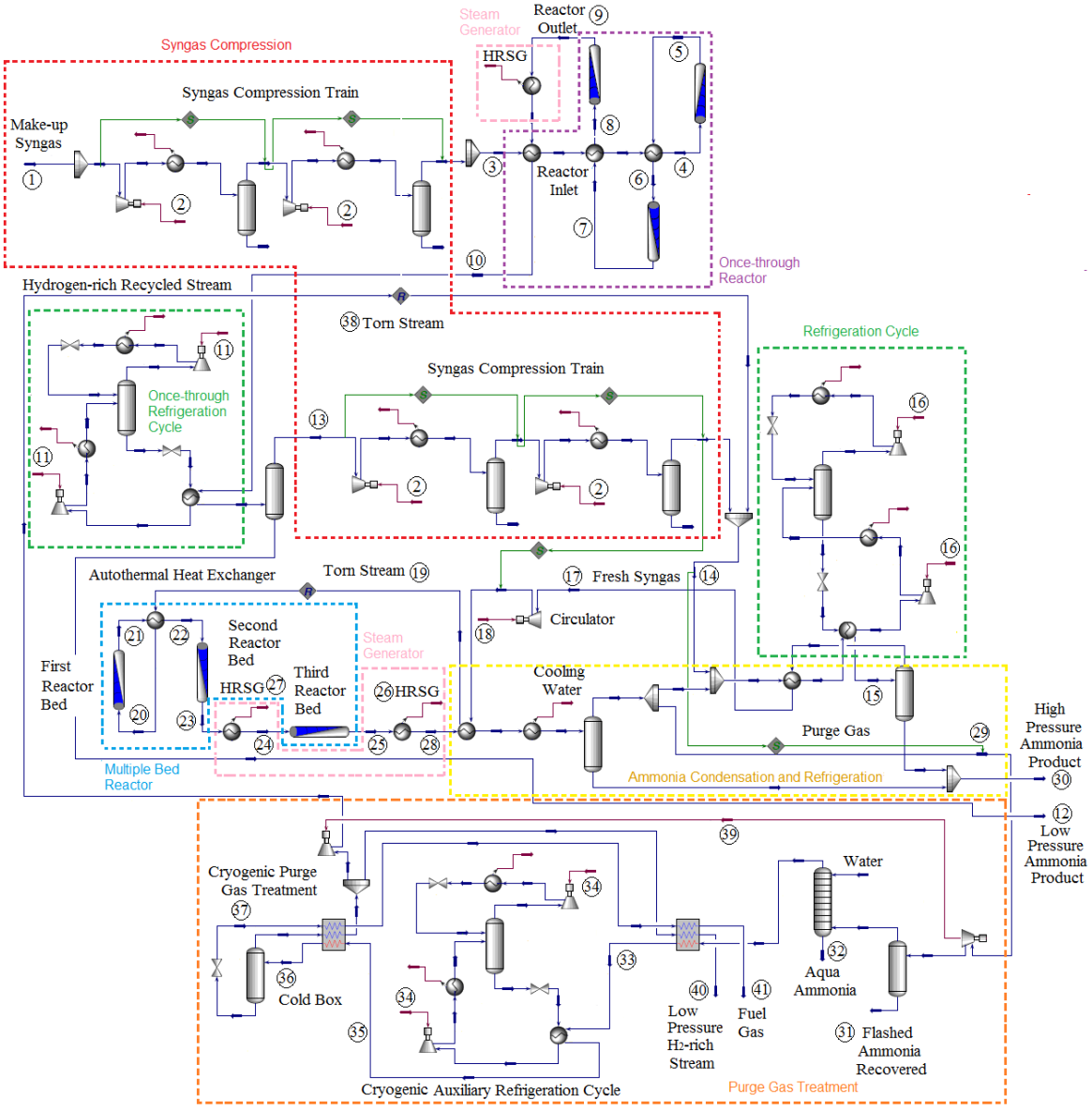

Fig. 2. Dual Pressure Ammonia Synthesis flowsheet (see also Table A.3).

Amongst the main advantages of the purge treatment process are (i) the removal of the inerts from the ammonia loop without appreciable loss of valuable hydrogen, (ii) the enhancement of the reactivity of

the system, which in turn reduces the size of the equipment, and (iii) the reduction of the power consumption in the syngas circulator and the refrigeration systems by recovering hydrogen and nitrogen at higher pressures [45]. According to some studies, the recovered hydrogen could be used to increase the production by approximately 4%, provided that incremental air and syngas compression capacities are available, or the equivalent energy savings on the original production capacities [46]. In the cryogenic method, purge gas is initially water scrubbed for ammonia removal, which otherwise would solidify downstream [40]. Ammonia could be distilled out of the aqueous mixture [25] or directly applied as a fertilizer [39], whereas the ammonia-free purge gas moisture is removed by means of molecular sieves [25, 47]. In the cryogenic section (cold box), refrigeration is supplied by the expansion of the separated liquid and additional chilling from an ammonia refrigeration system [33, 45], up to temperatures (-190°C) suitable to separate almost all the methane and argon contained in the purge gas stream [45]. Due to mechanical limitations on the brazed aluminum plate fin heat exchanger (PFHE), the recovery of the H_2-N_2 mixture from the purge gas is preferably carried out at pressures below 90 bar [47]. After the separation of vapor (basically N_2 and H_2) and liquid phases is performed, the former is reheated, and then the major part is recompressed at essentially the same pressure than that of the makeup syngas. Separated liquid is then reheated and used in the plant fuel system. The uncompressed fraction of the hydrogen-rich gas could be either externally recompressed and recycled to ammonia loop [41] or used as fuel in the ammonia plant [48]. It is important to point out that, in this work, it is considered that after the upstream methanator unit, the water content in the syngas is reduced to less than 0.2% mol at the inlet of the first compressor stage by using cooling water and a condensate separator. Then, water is considered as practically condensed out from the syngas along the compression train (< 0.06% in condensate separator), with any further trace of impurities being withdrawn with the condensed ammonia produced. For the low pressure case, molecular sieve units consisting of fixed bed absorbers working in alternate way and its respective regeneration system are commonly used, but these devices have not been explicitly simulated. For regeneration purposes, the molecular sieves may be heated up by a slip stream of the flue gas and the low pressure hydrogen-rich gas produced in the purge gas treatment unit. Other oxygen containing compounds that act as catalyst poisons, such as CO and CO_2, are assumed as totally converted to methane in the upstream methanation unit.

3. Methodology

The exergy method is used to assess the performance of the various components of the ammonia production unit. In the following sections, the process balances, exergy efficiency definitions and the Counteraction principle essentials are presented.

3.1. Process modeling

Mass, energy, exergy and economic balances of each sub-process under interest are carried out by the use of Aspen Hysys® V8.6 software. Since process streams in ammonia plants are complex multi-component/multi-phase systems, an enhanced SRK equation of state (EOS) in Aspen Hysys® based on the semi-empirical EOS of Redlich-Kwong with Soave modifications (SRK), is used to determine the thermo-physical properties of each flow present in the system. The volume translation concept introduced by Peneloux et al. [49] is used to improve molar liquid volume calculated from the cubic equation of state [50]. Proprietary enhancements are claimed to allow SRK method to handle high pressure systems with an extended range of applicability. Some improved binary interaction parameters were used in order to obtain the species fugacities in both phases to accurately calculate the vapor-liquid equilibrium (VLE) of non-condensable species in liquid ammonia [51]. Moreover, as

exergy calculation is not straightforward in the Aspen Hysys® environment, physical and chemical exergy calculations, as well as exergy efficiencies are assessed using VBA® scripts as *user defined functions* [52]. Aspen Hysys® is also used to assess the performance of the process components working under different loads and conditions, for predicting the energy demand of chemical processes and modeling systems involving complex chemistry, such as the ammonia reactor. Costs of the process streams and bare module equipment costs for the ammonia loop are calculated by using the methodology proposed by Turton et al. [53]. Finally, some indicators for estimating the performance of each configuration of the processing unit, which allow performing systematic comparisons between different designed setups, are proposed.

3.1.1. Process kinetics and equilibrium conversion

By considering the stoichiometry of the ammonia synthesis $N_2 + 3H_2 \rightarrow 2NH_3$, the nitrogen conversion rate for an adiabatic packed bed reactor (PBR) with no radial internal gradients operating at steady state, is calculated by the general Temkin-Phyzev correlation [54, 55] and the molar balance in terms of the reactor conversion ξ, the catalyst volume V (m^3) and the reaction rate r (kmol $m^{-3}_{cat}h^{-1}$) [56], according to Eq.(1):

$$n_{N_2,inlet}\frac{d\xi}{dV} = -r_{N_2} = k_b\left[K_P^2 f_{N_2}\left(\frac{f_{H_2}^3}{f_{NH_3}^2}\right)^{\alpha} - \left(\frac{f_{NH_3}^2}{f_{H_2}^3}\right)^{1-\alpha}\right] \tag{1}$$

where $\xi = \left(n_{N_2,inlet} - n_{N_2,outlet}\right)\Big/ n_{N_2,inlet}$, and $K_P^2 = k_f / k_b$ is the equilibrium constant calculated as suggested by [57]. Moreover, the fugacity of the component *i* at the partial pressure of the component in the system is approximated as $f_i = x_i \cdot f_i^{\circ} = x_i \cdot \gamma_i \cdot P$, where γ_i is the activity coefficient of component *i* calculated as in Dyson and Simon [54] and *P* the total pressure of the reactive system. Table 1 shows the reported pre-exponential Arrhenius factor and activation energy for the backward (*b*) reaction of ammonia synthesis based on proprietary catalyst data [55].

Table 1. Pre-exponential factor and activation energy for backward (*b*) reaction [55].

Parameter	**k_{0b}**	**Ea_b** (kJ/kmol)	**α**	**Observations**
Value	2.57e14	163500	0.55	Montecatini catalyst, *f* in atm.

On the other hand, the pressure drop along the reactor bed is calculated by using Ergun correlation, Eq.(2) [56]:

$$\frac{dP}{dz} = -\frac{G}{\rho D_p}\cdot\frac{(1-\phi)}{\phi^3}\cdot\left[\frac{150(1-\phi)\mu}{D_p} + 1.75G\right] \tag{2}$$

where $\phi = V_{Void}/V_{Bed}$ is the void fraction of the packed bed volume, ρ is the gas density, G is the superficial mass velocity of the reacting gases, and D_p is the catalyst diameter. Typical void fraction ranges from 0.33 to 0.5 [58], with lower values leading to larger pressure drops [56]. Since each plug flow reactor bed is considered as adiabatic, the conversion calculated at the bed outlet from the energy balance, ξ_{EB}, is given by Eq.(3) [56]:

$$\xi_{\substack{Energy\\Balance}} = \frac{\sum \Theta_i C_{p,i}(T - T_1)}{-\left[\Delta H_R^{\circ}(T_R) + \Delta C_p(T - T_R)\right]} \tag{3}$$

where $\Theta_i = n_{i,inlet} / n_{N_2,inlet}$ is the ratio between the molar flow of the reactant *i* to the molar flow of the *inlet* nitrogen; $C_{p,i}$ is the specific heat capacity of the *reactant i*; and *T* and T_1 are the product and reactant temperatures, respectively. The denominator is the reaction enthalpy at T, and T_R is the reference temperature used to calculate the enthalpy of reaction at the reference state (e.g. 298K and 1 atm). Since, the second term in the denominator is often negligible compared with $\Delta H_R^\circ(T_R)$, the operation curve of the adiabatic bed can be approximated by a linear function with a slope $\beta \approx \sum \Theta_i C_{p,i} / -\left[\Delta H_R^\circ(T_R)\right]$ in a ξ *vs.* *T* plot (Fig. 3). Accordingly, the conversion achieved at the equilibrium for the adiabatic reactor bed corresponds to the intersection of the equilibrium curve (r_{N2} = 0) and the adiabatic operation line. It is worthy to note that operating near the set of temperatures at which the maximum conversion is achieved for a given reaction rate (*locus of maximum conversion*) may help reducing catalyst volumes.

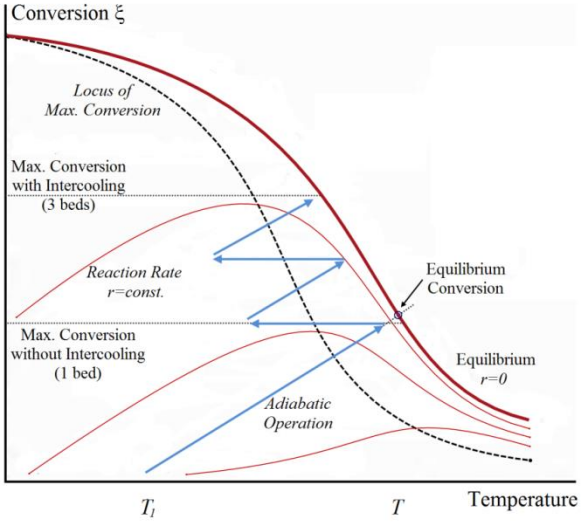

Fig. 3. Adiabatic operation lines, reaction rate contours and maximum conversion in an exothermic ammonia reactor [56].

In this work, it is assumed that the effectiveness factor of the small catalyst particles used (3 mm, bulk density 2300 kg/m^3, sphericity 1) is close to the unity, thus the reactants concentration inside the particles is closer to the bulk concentration. For the sake of simulating the reaction kinetics, the reactor effective volume is calculated by considering a cylindrical packed bed reactor (in contrast to non-circular cross-sectional configurations) and it is assumed that the axial diffusion effect diminishes with the increase of the flow rate in the channel. In other words, the model is simplified to a packed bed reactor (PBR) in Aspen Hysys® with a very fast radial mass transport and a large ratio of reactor to pellet diameter. The flow is assumed turbulent so that the rapid mixing of reactants is guaranteed. A more detailed resolution of the reactor simulation would be obtained by coupling the modeling of the non-linear reaction kinetics to the computational fluid dynamics, which would considerably increase the computational time without an appreciable variation of the whole loop results. Thus, a trade-off between the effect of the reactor performance and reasonable computational time frames is selected. Additionally, the effect of the catalyst aging in its activity variation remains out of the scope of this paper.

For lower to moderate pressures, the vapor-liquid equilibrium (VLE) of ammonia could be estimated by applying the Raoult's law and considering that condensed ammonia is almost pure in the liquid

phase (i.e. ideal solution), whereas the ammonia in equilibrium in the vapor behaves as in an ideal mixture of non-ideal gases [59]. However, for higher pressures and for species above their critical temperatures, the fugacity of the species *i* in the non-ideal liquid phase is more conveniently calculated in terms of the system pressure $f_i = x_i \cdot \phi'_i \cdot P$ (instead of in terms of their vapor pressure $f_i = x_i \cdot \gamma_i \cdot p_i$), especially for substances whose vapor pressure p_i may not be defined above their critical temperatures (such as dissolved hydrogen). The fugacity coefficient of species *i*, ϕ'_i, in both liquid (x_i) and vapor (y_i) phases is thus computed from the same equation of state (EOS), as well as the other thermodynamic properties such as densities, enthalpies and heat capacities [59].

3.1.2. Exergy calculation and exergy efficiency definition

The combination of the First and Second Laws of Thermodynamics led to the concept of *exergy*, which is defined as the maximum work that can be obtained by means of reversible processes from a thermodynamic system that interacts with the components of the environment at P_0 = 1atm, T_0 = 298.15 K until the equilibrium is attained [60]. Since exergy can be considered as a measure of the departure of the environmental conditions, it serves not only for defining indicators to assess the performance of chemical processes, but also as an indicator of environmental impact, taking into account both the efficiency of supply chain (from primary exergy inputs) and the efficiency of the production processes [61]. The total exergy can be divided into potential (P), kinetic (K), thermos-mechanical or physical (PH) and chemical (CH) exergy, however, the first two components can be generally neglected when compared to the physical Eq.(4) and chemical Eq.(5) components[60]:

$$B^{PH} = H - H_0 - T_0 \left(S - S_0 \right) \tag{4}$$

$$B^{CH} = n_{mix} \cdot \left[\sum_i x_i \, b_i^{CH} + R_u T_0 \sum_i x_i \, \ln \gamma_i \, x_i \right] \tag{5}$$

where x_i (or y_i) is the mole fraction of component *i* in the mixture, and b_i^{CH} is the standard chemical exergy of component *i*. The exergy balance of a control volume operating under steady state conditions is given by Eq.(6):

$$\sum B_{in}^{M} - \sum B_{out}^{M} + \sum B_{in}^{Q} - \sum B_{out}^{Q} + \sum W_{in} - \sum W_{out} = B_{Dest} \tag{6}$$

where B^M, B^Q and W are the exergy associated to the mass, heat and work interactions, respectively, and B_{Dest} stands for the exergy destruction due to the irreversibilities in the system. The share of exergy destruction owed to the highly exothermic chemical reaction processes can be calculated by Eq.(7) [62, 63]:

$$B_{dest,react} = T_0 \frac{dS_{gen}}{dt} = T_0 \left(n_{out} S_{out} - n_{in} S_{in} \right) = T_0 \int_{VC} \sigma \, dz = T_0 \int_{VC} r \, \frac{-\Delta G}{T} \, \mathrm{A} \, dz \tag{7}$$

where –ΔG/T is the chemical driving force. Eq. (7) integrates the contributions of the local entropy generation rates along the control volume, assuming local equilibrium conditions [64].

Due to the large recycle rates and low conversions in ammonia synthesis loop, the process gas involves a large amount of exergy in transit. This fact, along with the differences in process conditions and stream specifications renders the proposition of a general exergy efficiency definition not straightforward [60, 65-67]. The exergy efficiencies studied in this work can be classified in mainly two types: (i) *input-output* and (ii) *consumed-produced* efficiencies. The first type considers the ratio between all the exergy flows leaving the system and the exergy flows fed to it, whereas the second

type attempts to differentiate the exergy effectively consumed (or produced) by the system from the untransformed exergy by calculating the exergy change of specific streams on the way to product.
Notwithstanding its simple formulation, the *input-output* exergy efficiency, defined by Szargut et al. [60] as in Eq.(8), may provide misleading results as it deceptively assumes values close to unity for operations which, from an engineering point of view, have a poor performance [66, 68]. *Input-output* type efficiency can be even negative for some process [69]. Table 2 compares an *input-output* type, namely the rational exergy efficiency, Eq. (8), along with several exergy efficiency definitions, Eqs.(9-11), proposed for better evaluating the overall performance of the ammonia loop [70]. Since the exergies of the input and output material flows are much larger than the energy flows (i.e, the power consumption), the rational exergy efficiency leads to untruthfully high and similar values. This is worsened when attempting to define exergy efficiencies in large volume (bulk) chemical production systems with recycle streams. To overcome this, an alternative approach has been proposed first by Kirova-Yordanova [22], where the useful exergy of the material output is considered as *transit exergy*, subtracting it from the numerator and denominator of Eq.(9), Table 2. However, Eq.(9) must be used with care, since it considers that all the outlet material flow is exergy in transit, although a chemical reaction of the syngas occurs in the loop. Actually, according to Brodyansky et al. [67] only inerts could be regarded as *transit exergy* [69]. Equation (9) also assumes that all the non-reacted nitrogen and hydrogen is recycled back to the ammonia converter and thus liquid ammonia, methane and argon are the only material exiting the system.

Table 2. Comparison among the exergy efficiency definitions of the overall ammonia synthesis unit.

Definition	**Formula**
Rational (8)	$\eta_{Rational} = \frac{B_{useful,output}}{B_{input}} = 1 - \frac{B_{Dest}}{B_{input}} = 1 - \frac{B_{Dest}}{\left(B_{\substack{Makeup \\ Syngas}} + B_{BFW}^{PH} + W_{Total} \right)}$
Transit (9)	$\eta_{\text{Transit}} = \frac{\left(B_{useful,output}^{Total} - \mathbf{B}_{\mathbf{useful,output}}^{\mathbf{Material}} \right)}{\left(B_{input}^{Material} - \mathbf{B}_{\mathbf{useful,output}}^{\mathbf{Material}} + B_{input}^{Exergy\ Flow} \right)} = \frac{B_{Steam}^{PH}}{\left(B_{\substack{Makeup \\ Syngas}} + B_{BFW}^{PH} - \left[B_{Ammonia} + B_{Inerts} \right] + W_{Total} \right)}$
Recovered (10)	$\eta_{\text{Recovered}} = \frac{B_{Recovered}}{B_{Consumed}} = \frac{\left(B_{Steam}^{PH} - B_{BFW}^{PH} \right)}{\left(B_{Makeup\ Syngas} - \left[B_{Ammonia} + B_{OffGas} \right] + W_{\text{Total}} \right)}$
Relative (11)	$\eta_{\text{Relative}} = \frac{B_{Consumed,\ ideal}}{B_{Consumed,\ actual}} = \frac{B_{Ammonia}}{B_{Makeup\ Syngas} + B_{BFW} + W_{Total}}$

Due to the shortcomings of the previous exergy definitions and by considering the process technical limitations and the exothermic characteristics thereof (e.g. need for intercooling, kinetics, etc.) [62], in this work, a more appropriate way to calculate the loop performance is proposed. Since the enthalpy of ammonia synthesis is about 8.8% (2.718 MJ/tonNH_3) of the total consumption of the integrated syngas and ammonia plant, there is a strong incentive in recovering as much as possible of this waste heat [34]. Accordingly, by considering an *ideal* case in which all of the exergy input neither embodied in the ammonia nor in the off-gas products is recovered in the form of steam (see Eq.(12)), a new efficiency definition, Eq.(10), Table 2, can be proposed [70]:

$$B_{Dest} = 0 \quad \rightarrow \quad B_{Steam} = B_{Makeup\ Syngas} - \left[B_{Ammonia} + B_{OffGas} \right] + W_{\text{Compressor}} + W_{\text{Circulator}} + W_{\text{Refrigeration}} - B_{BFW} \qquad (12)$$

Eq.(12) impose a limit for the maximum exergy recovery in the form of steam, when pressure drop ($W_{\text{Circulator}} \to 0$) and process irreversibility ($B_{Dest} \to 0$) tends to zero. Since the exergy difference and not the total mass flows are written in Eq.(10), the difficulties presented when defining the exergy efficiency of large recycle systems can be overcome. On the other hand, Eq.(10) is evaluated in terms of the exergy recovery potential. However, by realizing that the main objective of the chemical unit would be rather to produce ammonia, instead of expending the valuable incoming exergy of the makeup syngas in producing lower quality exergy of steam, in this work, a second exergy efficiency definition is introduced. Equation (11) is calculated as the ratio of the minimum exergy consumption in ammonia production (i.e. the ammonia chemical exergy, 327,000kJ/kmol) to the actual loop consumption. Since the denominator of Eq.(11) includes the exergy of the material flow rate of the makeup syngas, this definition is slightly less sensitive to the loop parameters, such as recycle/purge ratio, refrigeration duty and pressure drop, all of them represented by the total power consumption term. Anyhow, Eq.(11) gives a measure of the overall potential of improvement of the loop when compared with the minimum exergy requirements for ammonia production from nitrogen and hydrogen. It is clear that this value can be much lower if the boundaries of the system are extended for including, for example, the front-end syngas production process.

Table 3 shows the proposed exergy efficiency definitions for representative components of the ammonia unit. In Table 3, the *input-output* definitions for the individual loop components are not defined due to their impractical use. Some processes with unpractically reduced driving forces may seem to be efficient, even if its industrial performance is questionable. In Eq.(14), the exothermic ammonia converter efficiency is defined in terms of the increase of thermal exergy of the reactor effluent at the expense of a fraction of the chemical exergy of the reactants [37].

Table 3. Consumed-produced exergy efficiency definitions for representative equipment.

Unit (Eq.)	**(a) Consumed-Produced**
Syngas Compression (13)	$\eta_{\text{Comp,CP}} = \dfrac{\left(B^{PH}_{Compressed\ \ Syngas} - B^{PH}_{Makeup\ \ Syngas}\right)}{W_{Comp} + W_{\substack{Cooling \\ Tower}}}$
Ammonia Reactor Bed (14)	$\eta_{\text{Reactor,CP}} = \dfrac{B^{PH}_{Reactor\ Product} - B^{PH}_{Reactor\ \ Feed}}{\left(B^{CH}_{Reactor\ \ Feed} - B^{CH}_{Reactor\ Product}\right)}$
Refrigeration cycle (15)	$\eta_{\text{Refrigerator,CP}} = \dfrac{-Q_{\text{Evaporator}}\,(T_0/T_{Evaporator} - 1)}{W_{\substack{Compressor\ I \\ Compressor\ II}} + W_{\substack{Cooling \\ Tower}}} = \dfrac{COP_{\text{actual}}}{COP_{\text{Carnot}}}$
	$\eta_{\text{Refrigerator, CP2}} = \dfrac{B^{PH}_{Syngas,in} - B^{PH}_{Syngas,out}}{W_{\substack{Compressor\ I \\ Compressor\ II}} + W_{\substack{Cooling \\ Tower}}}$
Heat recovery Steam generator (16)	$\eta_{\text{HRSG,CP}} = \dfrac{\left(B^{PH}_{Steam} - B^{PH}_{BFW}\right)}{\left(B^{PH}_{Hot\ Process Gas} - B^{PH}_{\text{Cold }Process\,\text{Gas}}\right)}$
Cryogenic Purge gas Treatment (17)	$\eta_{\text{CryoPG}} = \dfrac{B^{PH}_{\substack{Low\ Pressure\,H_2-N_2 \\ mixture}} + B^{PH}_{\substack{High\,Pressure\,H_2-N_2 \\ mixture}} + B^{PH}_{Fuel\ Gas}}{B^{PH}_{\substack{Ammonia\ Free \\ Purge\ Gas}} + B_{\substack{Scrubbing \\ Water}} + W_{\substack{Aux. \\ Refrigerator}}}$

In Eq.(15), two approaches are considered for the refrigeration cycle. Differently from the first approach (CP), the second efficiency (CP2) includes the irreversibilities in the control volume of the evaporator, thus $B^{PH}_{Process Gas}$ stand for both the inlet and outlet refrigerated process gas.

3.1.3. Counteraction principle: application to the ammonia synthesis.

Pressure variations drastically affect the thermodynamics and economics of the ammonia synthesis. According to Le Chatelier Principle [37, 71], while higher loop pressures simultaneously increase the ammonia equilibrium conversion and reaction rate (thus increasing the available enthalpy of reaction for steam production), it also increases the syngas compression, along with the required equipment cost and reliability (but lowers the circulation duty). Higher pressures also allow reducing the refrigeration power and improve the ammonia separation process, reducing the equipment size. On the other hand, if ammonia synthesis is carried out at lower pressures (and consequently, lower temperatures), the enthalpy of reaction is not anymore available for high pressure steam generation, and the usefulness of this low grade temperature reactor effluent may be doubtful [36]. However, if the pressure is reduced the process irreversibilities are also reduced according to the Counteraction Principle. This decision criteria leads to diametrically opposite, conflicting objectives [37], namely the reduction of the exergy losses by reducing the driving force of the process and the increase of the process yield by increasing it. This concept is better shown if all the reaction enthalpy is considered as isothermally removed at T_0 as ammonia is produced [9]. For a mixture of ideal gases, the exergy efficiency in terms of the exergy pressure component would be given by Eq. (18):

$$\eta_p = \Delta B^{PH} / \Delta B^{CH} = \frac{\left(n_P - n_R\right) R T_o \ln(P_P / P_R)}{\Delta B^{CH}}, \quad \text{for } n_P < n_R \tag{18}$$

In other words, the exergy efficiency of isothermal reactions that decrease in volume may actually increase as the pressure is reduced, since the pressure exergy of the products exceeds the pressure exergy of the reactants [37]. To tackle this dilemma, it could be considered: (i) to reduce exergy losses by avoiding the reactions to run into completion [37], shifting the multibed reactor away from equilibrium by producing high pressure steam; while (ii) introducing novel dual pressure ammonia loops (e.g. Udhe Dual process), that operates by starting at lower pressures and proceeds at higher ones. Those systems have been claimed to increase exergy efficiency and still maintain high production rates. Thus, the Counteraction principle is used to drive the process irreversibilities down by using incremental levels of pressure in the ammonia production processes, while the reduction of the recycle rates allows cutting down the energy required in the circulation and refrigeration systems.

4. Results and discussion

Next, the performance of two loop configurations of ammonia synthesis, one operating at a single pressure and the other under the dual pressure configuration, are compared in terms of the exergy consumption, reactor conversion, exergy efficiency and exergy destruction rates in the various units.

4.1. Comparison between single and dual pressure loop parameters.

Table 4 compares the processes parameters of the single and dual pressure unit configurations. For the single pressure configuration at 150 bar (SP150), the total power consumed in refrigeration is about 69% higher than that of the dual pressure system (DP). The circulation power is also considerably higher, as a direct consequence of a 76% larger recycle flow rate and higher loop pressure drop. The loop reactor conversion is, thus, reduced in about 20.2% compared with the DP, followed by a decrease in the amount of steam produced. Since in the DP unit an important percentage of the inert and the ammonia converted is withdrawn before reaching the loop system, the compression power consumed in the syngas compressor can be reduced, along with the recycle rate as well as the cooling

water requirements. The main advantage of the DP system over the SP150 and SP200 configurations does not only arise from the point of view of economics (higher revenues), but also from a higher exergy efficiency and other desirable characteristics, which renders the DP synthesis more attractive in terms of investment and feedstock economy as well as in mitigating the environmental impact. Even though the DP system has lower recycle inerts, higher recycled amounts of ammonia compared with the SP200 configuration slightly reduces the reaction conversion of the loop. It is also worthy to notice that, even though an additional refrigeration duty (827kW) downstream the once-through reaction section is required, the addition of a low pressure ammonia separation system reduces the required refrigeration duty of the loop section by 58.6% and 34.6% compared with the SP150 and SP200 configurations, respectively. It is also striking that, even if an important amount of the makeup syngas must still be compressed to levels of pressure comparable to those of SP200 system, the total exergy consumption required in the syngas compression train in the DP configuration is almost the same that the consumed in the SP150 system. In this way, the more favorable kinetic and equilibrium conditions and ammonia separation characteristics at higher pressures can be exploited, and at the same time, the losses associated to the compression and the safety and control issues related to the high operating pressures can be minimized.

Table 4. Main process parameters of the various loop configurations.

	Single Pressure (SP)		**Dual Pressure (DP)**
Process parameter	**150 bar**	**200 bar**	**83-200bar**
Once-through reactor inlet temperature T_{OT} (ºC)	--	--	290
First bed gas preheating temperature, T_1 (°C)	365	310	350
Third bed inlet gas temperature, T_3 (°C)	400	380	400
Once-through reactor pressure drop (bar)	--	--	0.32
Loop reactor pressure drop (bar)	3.6	1.3	0.70
Makeup syngas H_2/N_2 ratio	2.94	2.91	2.91
Fresh syngas H_2/N_2 ratio	2.99	3.00	2.99
Inerts mole fraction (%)	1.40	1.40	1.40
Makeup syngas water molar fraction (%)	0.2	0.2	0.2
Recycle ammonia composition (%)	2.22	1.81	**3.88**
Recycle inerts composition (%)	10.86	7.43	8.29
Recycled reactor feed H_2/N_2 ratio	2.86	3.08	2.98
Recycle molar flow rate (kmol/h)	20,979	15,412	**11,933**
Fresh syngas compression power (kW)	8,193	9,954	**8,516**
Once-through refrigeration power (kW)[1]	--	--	827
Loop refrigeration power (kW)[2]	4,890	3,090	2,022
Cryo. Auxiliary refrigeration power (kW)	35.6	39.7	39.4
COP Carnot refrigeration	4.42	4.42	4.42[3]
COP actual refrigeration	2.43	2.43	2.43[3]
Circulator power consumption (kW)	498	101	42,9
Purge gas fraction (%)	7.0	7.0	7.0
Once-through reactor conversion (%)[4]	--	--	29,3
Loop reactor first bed conversion (%)[4]	17.4	24.5	20.9
Loop reactor second bed conversion (%)[4]	6.1	8.2	9.3
Loop reactor third bed conversion (%)[4]	5.7	9.1	7.5
Reactor conversion (%)[4]	26.8	37.1	33.6
Waste heat recovery rate (kW)[5]	28,379	29,518	31,482
Cooling water – gas condensation (kmol/h)[6]	28,948	34,846	27,571

Cooling water – refrigeration cycle (kmol/h)[6]	330,894	210,283	239,202[7]
Scrubbing water consumption (kmol/h)[8]	135	100	100
Aqua ammonia production (m^3/h)[9]	2.25	2.28	2.25
High P, H_2-rich recovered stream (kmol/h)[10]	86.8	146.2	145.9
Low P, H_2-rich recovered stream (kmol/h)	74.0	46.2	32.0
Fuel gas production (kmol/h)[11]	88.64	89.2	85.1
Incomes ($/ton NH_3)[12]	637.2	644.5	643.4
Costs ($/ton NH_3)[13]	403.1	402.7	397.8
Revenues ($/ton NH_3)	234.1	241.8	**250.8**
Annualized Bare Module Cost ($/ton NH_3)[14]	23.8	26.3	25.8

1). Condenser pressure: 13.6 bar, evaporator pressure: 424.4 kPa. Minimum temperature approach: 5ºC. 2). Condenser pressure: 13.6 bar, evaporator pressure: 115.2 kPa. Minimum temperature approach: 5-10ºC; 3). Except for the once-through section refrigeration, whose values are COP_{actual} = 5.2 and COP_{Carnot} = 10.9; 4). Reactor conversion ξ as defined in Section 3.1.1; 5). Saturated steam as 100 bar; 6). Cooling water maximum outlet temperature: 35-40°C; 7). Condenser water cooling duty: 57% loop refrigeration, 42% once-through refrigeration, 1% cryogenic unit auxiliary refrigeration; 8). Water at 30ºC and 79.5 bar; 9). Ref. [39]; 10). Hydrogen recovery efficiency > 93.11 % - 94.92%; 11). Methane 26.5%-31.7%, Nitrogen 52%-57.5%; Argon 8.0%-8.5%; 12). Ammonia price: $32/GJ; 13). Natural gas cost: $9.7/GJ. Annualized bare module cost included; 14). Interest rate 6%, lifespan 20 years. CEPCI: 550 (2010) [53, 72].

For each operation configuration, similar amounts of fuel gas are produced (26.5%-31.7% CH_4, 52%-57.5% N_2 and 8.0%-8.5% Ar), whereas the higher hydrogen recovery rates occur at both SP200 and DP configurations. However, it must be observed that, in the DP case, the proportion of hydrogen-rich stream recovered at basically the same loop pressure is 80.2%, while for the SP150 and SP200 those proportions are appreciable lower (53.9% and 75.9%, respectively). In this way, the use of a cryogenic purge gas treatment unit in combination with a dual pressure reaction system helps improving the utilization of the energy of the natural gas consumed in the ammonia production process. Moreover, argon, nitrogen and methane may be separated by cryogenic distillation or permeable membranes, to further increase the overall efficiency. According to Table 4, in the SP150 and SP200 configurations, the makeup syngas compression consumes almost 56.7% and 75.5% of the power supply, respectively, followed by the refrigeration cycles (39.8% and 23.7%, respectively) and the circulator (<3.4%). It is important to notice that the total power consumption (compression, refrigeration and circulation) in the DP configuration reaches 10.6MW, i.e. 24.1% and 35.9% lower than in the other systems. Some authors reported that given the compressor and circulator efficiencies and the pressure drop through the loop, a pressure-independent power consumption for operating pressures between 140-315 bar, with a flat minimum in 155 bar, is obtained [33]. Other studies have found higher values (180-220 bar) [42]. Those claims may be partially verified from the results shown in Table 4. The total power consumption in the synthesis units studied (including fresh syngas compressor, refrigeration compressors and circulator) is found to vary between 10,620 kW and 14,444 kW. Thus, even if the power consumption for both SP configurations differ only about 9% from each other, relatively higher energy consumptions are found when compared to the DP configuration (i.e. 19% and 25% higher at SP200 and SP150, respectively). Finally, it is pointed out that dual pressure processes have been indeed proposed to operate at larger ammonia production capacities, taking advantage of the economy of scale. Lippman *et al*. [31], reported that by comparing the specific production costs based on the same depreciation, feedstock and manufacturing costs, the ammonia production cost per ton is 11% less in a 3300t/day plant integrating the dual pressure system than a conventional 2000t/day plant.

4.2. Reaction kinetics: the multibed catalytic reactor with intercooling

The conversion *vs*. temperature plot shown in Fig. 4 is a graphical representation of the relation between the kinetics operation parameters of the multibed catalytic reactor (e.g., bed feed temperature, conversion and reaction rate) and the indirect cooling system. These figures correspond to the kinetics characteristics of the Montecatini catalyst reported in Table 1. The contours of the constant reaction rates, the approach to the equilibrium and the adiabatic reactor lines have been determined for each one of the configurations studied (Table 4). Due to safety issues and metallurgical limitations for high pressure, hydrogen-rich operation conditions, the maximum reaction temperatures are limited to about 550ºC. Meanwhile, the risk of poisoning by even low O_2 concentrations sets a practical lower bound to the catalyst temperature to about 290°C [33].

The relevance of the study of the kinetics of the ammonia reaction process together with the exergy method relies on the fact that, even though avoidable exergy destruction in reaction is generally small, the exergy destroyed on the other components (compressors, heat exchangers, separators, etc.) will strongly depend on the reactor performance [73, 74]. For instance, fixed the production capacity, the specific exergy consumption depends on the allowable space velocity and the conversion rate which, in turn, depends on the catalyst activity and the reactor size.

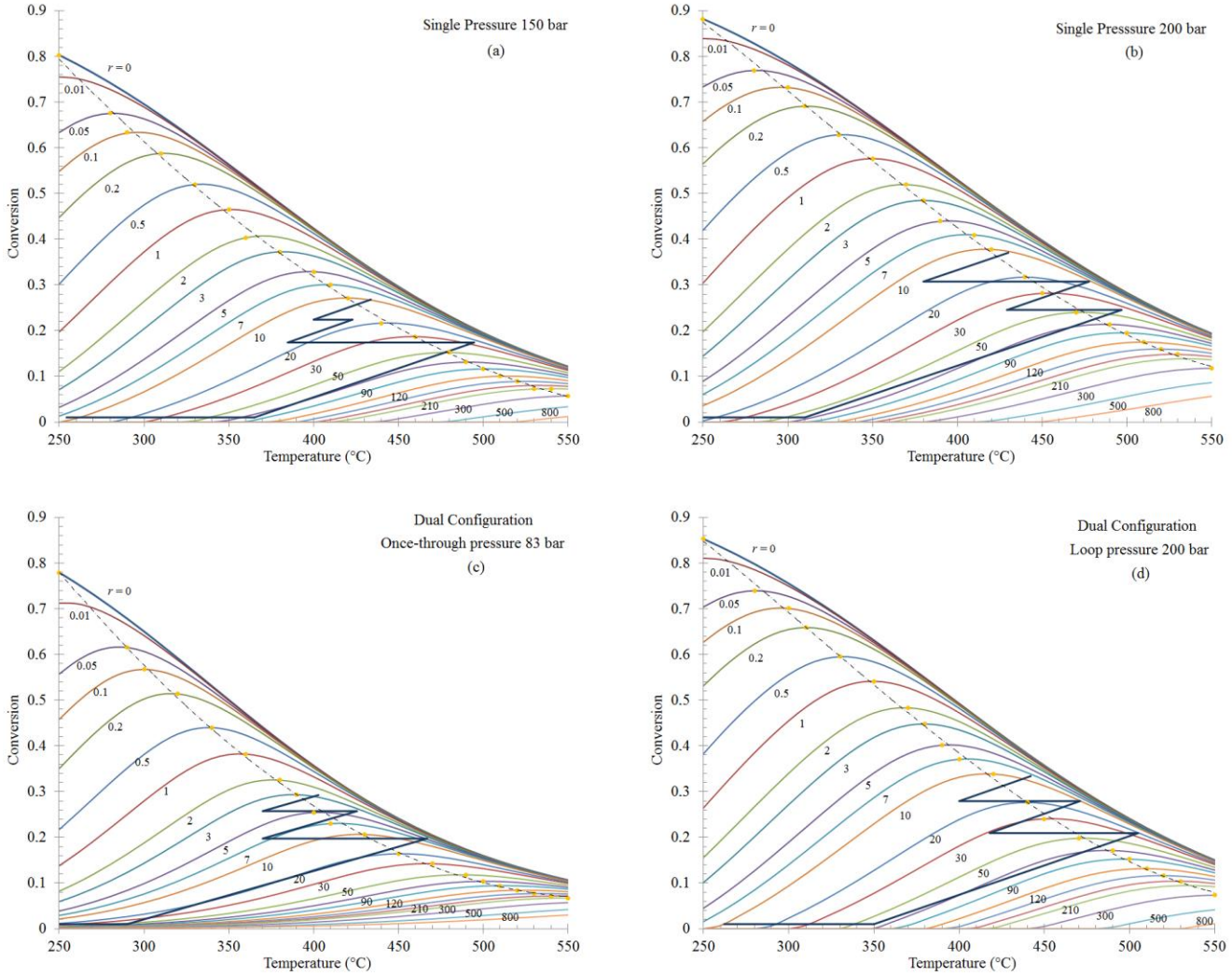

Fig. 4. Conversion *vs.* Temperature plot. The contours of constant reaction rates are given in kmol m^{-3} h^{-1} (a) Single pressure 150 bar, (b) Single pressure 200 bar, (c) Dual configuration, once-through pressure 83 bar, (d) Dual configuration, loop pressure 200 bar.

Besides, the lower the space velocity, the closer the equilibrium may be attained, thus implying a higher conversion rate. On the other hand, by increasing the circulation rate, higher amounts of ammonia could be produced at expense of lower conversions per pass, reducing the reactor irreversibilities [32]. However, the circulation rate cannot be increased indefinitely since the autothermal ignition temperature of the converter might not be attained (Fig. 4), and also the exergy losses due to pressure drop would rise disproportionately [32, 74]. Lower conversion also entails larger equipment and, consequently, higher capital costs. Accordingly, Figs. 4(a-d) may be used to determine the concentration-temperature distribution that allows the SP200 and DP configuration to attain a higher conversion but also reduced irreversibilities associated to the reacting driving force. As discussed in previous works [74], even though the adiabatic reaction lines in Fig. 4 closely follow the *locus of maximum conversion rates*, the reactor irreversibilities arisen from the higher conversions are compensated by the enhancement of the performance of the integrated chemical unit. It is important to clarify that, even though a once-through ammonia converter working at a higher pressure may allow reducing the required catalyst volume, the concentration of the reagents would be so high, or equivalently, the amount of inerts entering such system would be so low (compared to the 8% inert + 2.5% ammonia content in the SP200 feed), that an auxiliary ammonia injection system would be required to moderate the exit temperatures due to extremely high conversion rates [31, 32]. This certainly would introduce another source of system irreversibilities, not only because ammonia is mixed to the reacting system but also because it inevitably would trigger some hindering effects in the reaction conversion and the compression system. Accordingly, the low pressure characteristics offered by the once-through reaction section proves to be thermodynamically limited to an acceptable temperature, avoiding the need of ammonia injection [31, 32].

Differently from other reactors using direct cold shot [75] or autothermal reactors [76], the indirect cooling system depicted in Fig. 4 has gained preference as it allows producing high pressure steam. Further works discussed the advantage of a Dowtherm cooled-reactor system [73, 77], but according to Johannessen et al. [64], a cooled-reactor would result more difficult to control and increase the capital cost. Actually, the optimal configuration would rather require a separated adiabatic reactor operating in *reaction-mode* followed by a diathermic one operating in *heat-exchange-mode* [63]. Thus, it is beneficial in terms of economics and energy efficiency to split the operation into separated sets of one or more adiabatic reactor stages with intercooling, as shown in Fig. 4. In this way, a more complex optimal control problem can be reduced (or avoided), and the search of an optimum design can be simplified [63, 74].

4.3. Exergy destruction and efficiency of representative equipment

Figure 5 shows the overall exergy efficiency of the various unit configurations as defined by Eqs. (9-11).

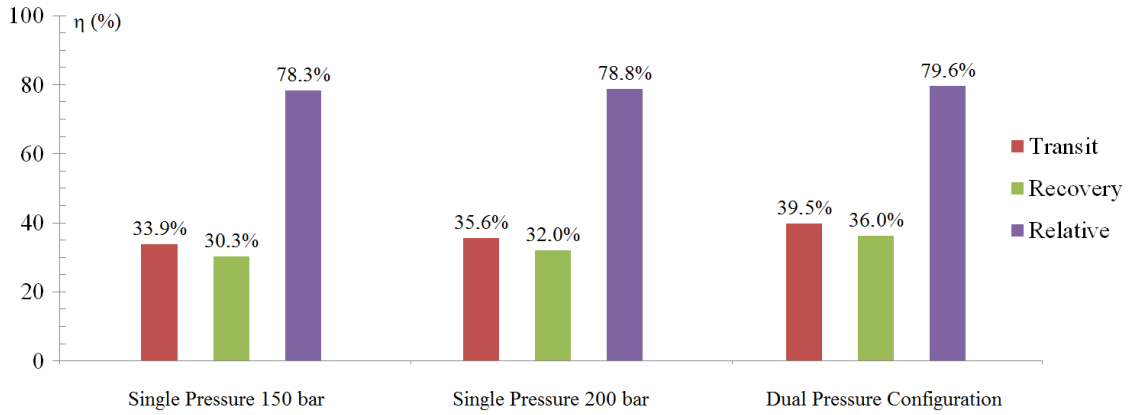

Fig. 5. Overall (plant-wide) exergy efficiencies for the various ammonia configurations.

As expected, *rational* efficiency, Eq.(8), attains values above 91%, showing to be insensitive to the variation of the process parameters. Thus, it is not considered as a reliable indicator of the exergy performance. Contrarily, Eqs.(9-11) are more sensitive since they only take into account the effect of the loop parameters on the performance of the chemical process. In the following, the causes of the low exergy performance and suitable alternatives for improving the exergy efficiency are discussed.

Transit efficiency definition is slightly higher than the recovery efficiency since, as mentioned in section 3.1.2, it assumes that all the non-reacted nitrogen and hydrogen is recycled back to the ammonia converter and only liquid pure ammonia, methane and argon exit the loop. In other words, neither offgas production nor low pressure hydrogen-rich stream are considered. Besides, the term B_{BFW}^{PH} in Eq. (9) is considered as an input exergy quantity, and not as transit exergy in the waste heat boiler. The numerator in Eq.(9) has been originally proposed in terms of the electricity generated in an additional energy conversion process, e.g. an associated Rankine cycle (100 bar) [22]. However, in this work, the boundaries of the system studied are restricted to the steam generation process. The reason is that the recovery of the reaction enthalpy in the form of steam is actually linked to a more complicated combined steam and power production system in the integrated syngas and ammonia production plant, as described in Ref. [70]. Furthermore, fixed the available header pressure levels in the steam network system, there is not necessarily a direct relation between the power cycle performance and the ammonia loop parameters, since the steam system should be able to compensate the heat recovery network deficit. Accordingly, the loop performance and the available steam generation potential are suitably estimated by the *recovery* efficiency definition, which attempts to determine the opportunity to recover all the dissipated heat to the extent of the process limitation (i.e. an exothermic, equilibrium and rate limited, high temperature reactive system), in the form of a valuable ammonia unit subproduct, namely, high pressure steam. Dual pressure-based ammonia loops configuration, with a stepwise, increased reactor conversion and reduced loop recycle rates seems to perform better as concerns the reaction enthalpy recovery. In fact, increased system pressure and temperature also increases the exergy available in the process gas and the high pressure steam production is improved, as it can be inferred form the comparison between the recovery efficiencies of the SP units.

On the other hand, the *relative* efficiency has been defined by using the minimum theoretical exergy consumption required to produce ammonia from the elements in the environment. As such, the relative efficiency accounts for the maximum potential of energy savings, including the upstream production processes of nitrogen and hydrogen. But, notwithstanding its broader scope and improved sensitivity compared to the abnormally higher rational efficiency, this indicator still presents part of the

shortcomings posed by the efficiency definitions of bulk chemicals production processes with large flow rates. In an attempt to differentiate between the transiting exergy and the consumed exergy, Sorin and Paris [78] defined the 'transiting exergy in the utilizable stream'. They calculated it as the part of the exergy entering a unit operation and traversing it without undergoing any transformation, leaving the system with the 'utilizable stream'. However, due to the fact that the main loop effluent, namely the ammonia produced, has been actually transformed, apart from the small amount of feedstock in the purge and the traces dissolved in ammonia, no other stream cannot be considered as *transit exergy*.

Regarding Fig. 6, the principal irreversible phenomena that occur in the ammonia converter and steam boilers are the highly irreversible reactions and the finite temperature difference at which heat is transferred between the hot gases and the heated stream, respectively. Moreover, since the exergy associated with unreacted feed or inerts typically constitutes transiting exergy in the reactor volume [68], the high circulation rates and lower per-pass conversions in ammonia reactor render its exergy efficiency much lower than that of other industrial exothermic reactors [70, 79]. Despite the fact that most of the irreversibility due to chemical conversion is inevitable, exergy loss can still be reduced by preheating the reactants [60], or as in the present study, performing the chemical reaction at lower pressures without attaining the completion. This discussion will be extended further below. It also is interesting to remark the difference in the results obtained from the two exergy efficiency definitions for the refrigeration cycles. Since the *consumed-produced* efficiency CP2 includes the exergy destroyed in the control volume of the evaporator, the exergy efficiency is appreciable lower.

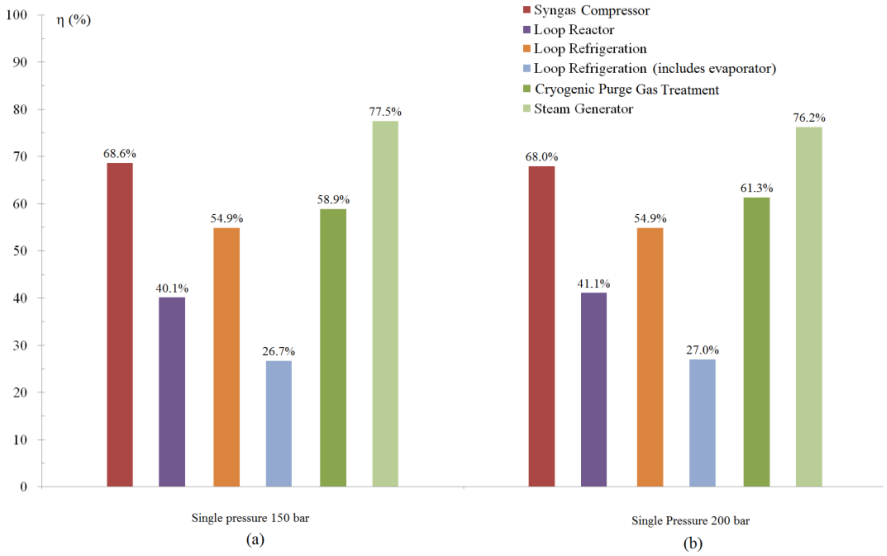

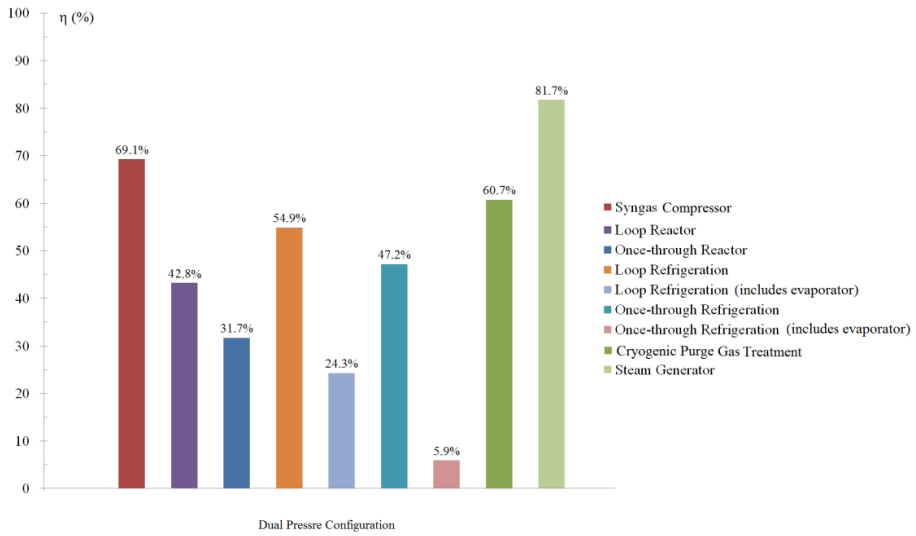

Fig. 6. Exergy efficiencies (*consumed-produced*) for representative components of the ammonia loop: (a) single pressure 150 bar, (b) single pressure 200 bar, (c) dual pressure configuration.

Regarding to the syngas compressor, the *consumed-produced* exergy efficiency is quite similar for any configuration. Moreover, it is not surprising that the exergy efficiencies in the refrigeration cycle are similar in all the cases, considering that the isentropic efficiency of the refrigeration compressors is equal, and the compression ratios are selected to reduce the refrigeration power consumption. Finally, even though no chemical reactions are present in the cryogenic purge gas recovery unit, other dissipative components lead to an exergy efficiency much lower than that expected by the simpler *input-output* definition. The throttling process of the cold-box liquid effluent (whereby it partially vaporizes generating the refrigeration driving force), the large temperature differences between the feed and exit streams in the cryogenic heat exchangers (ranging from 40°C to -191°C), and the auxiliary refrigeration system [45] are examples of those components. Figs. 5 and 6 suggest that more sensitive calculations of the exergy performance are attained when the goal of the unit/component and its dependency to the loop parameters is unequivocally defined, especially in the case of recycling systems with a relatively large mass flow input. In the same way, a better understanding of the system irreversibilities can be achieved by identifying the main components tasks, with the reactor performance playing the most important role in the ammonia loop. Figure 7 depicts a mechanical heat pump analogy of the exothermic adiabatic reactor, where the mechanical work replaces the chemical work. This representation helps to visualize the ways in which the energy available (exergy) in the chemical system can be totally or partially transformed to increase the physical exergy of the reactants [80, 81]. In Fig. 7, the recovery of the variation of the chemical exergy as work can be maximized by using a set of van't Hoff equilibrium boxes devised to carry out the reaction reversibly, where the chemical species interact only with the ambient while exchange heat and produce net work [82]. The maximum work recovery entails the full exploitation of the energy of the chemical reaction (Gibbs free energy) and the energy of mixing in a lesser extent [83]. Thus, if the reactor operation is performed reversibly, the variation of the chemical exergy equals the variation of the physical exergy between the reactants and products. In order to achieve this, a set of reversible heat pumps, operating between T_H and T_L and at infinitesimal temperature differences in the evaporator and condenser, ensure the reversible conditions. As long as no irreversibilities occur, the reactor exergy efficiency equals the unity, Eq.(14).

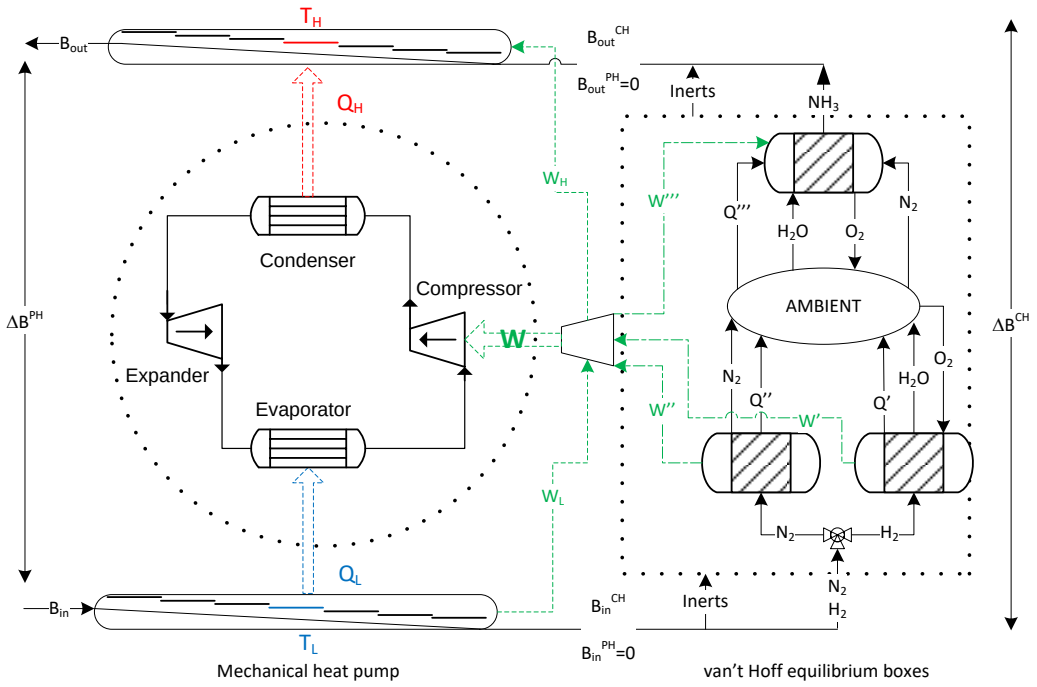

Fig. 7. Exothermic reactor represented as a chemical exergy-driven heat pump. Q', Q'' and Q''' represent the reversible heat rates transferred to the ambient at the reference temperature for calculating the maximum net chemical power done by the species (W', W'' and W''') in a set of van't Hoff equilibrium boxes.

However, in actual reactors, the chemical exergy consumed in the system is not entirely transformed into an equivalent form of work (i.e. variation of physical exergy) because of the spontaneous change in composition, diffusion, pressure drop and heat transfer between species. In Fig. 7, the exergy destroyed in the reactor is accounted for by the continuous release of the enthalpy of reaction in the uncontrolled form of internal energy, followed by the heat transfer from the hot products to the fresh reactants [81]. A mechanical analogy of such disordered transfer modes in opposition to a reversible heat pump would be an electric resistance or a mechanical stirrer used to partially convert the chemical exergy of the reactants into exergy of heat available at high temperature T_H. The increase of the physical exergy by using the latter methods cannot be used to reverse the chemical reaction in the van't Hoff box, differently from the case of the reversible heat pump, because the energy quality has been degraded. Bringing back the system to the initial state would require a footprint in the ambient, or equivalently, more fuel is required to reverse the chemical process. This represents a deeper insight of the exergy analysis when compared with the First law analysis.

Roughly, the exergy destruction contribution of the reaction relies on the equilibrium approach: the more complete the reaction, the higher the exergy destroyed [37]. On the other hand, the heat exchange and pressure drop related irreversibilities rely on the total conversion per pass: the higher the conversion, the lower the flow rate of the recycled, unreacted syngas and inert build-up. In fact, even though a large portion of the exergy inlet to the reactor is neither transformed nor destroyed along its volume, the *transit exergy* associated to it (a mixture of reactants, products and inerts) largely modifies the reactor performance. Consequently, the amount of exergy consumed in the condensation, refrigeration and circulation systems is also affected, not to mention the effect on the increased pressure drop, higher equipment sizes and space velocities and lower residence times. Lower

conversions also lead to increased hydrogen content in the purge gas stream, and thus to a higher exergy destruction rate in the purge gas treatment unit and to an improper feedstock utilization.

Denbigh [62] and Hinderink et al. [80] estimated the reactor irreversibilities for the ammonia oxidation and hydrogen production processes, respectively, in a chemical reactor operating at constant pressure and temperature by using Eq. (19):

$$B_{dest} = T_o S_{gen} = -T_o \frac{\Delta G_{reaction}}{T_{reaction}} \tag{19}$$

which is called the 'unavoidable lost work' or 'dissipated energy' and only can be used when the enthalpy of reaction is recovered as mechanical work at the constant temperature of reaction $T_{reaction}$. In the adiabatic reactor studied in this work, both pressure drop and temperature variation occur. Therefore, the maximum work given by the Gibbs energy function is not equivalent to the maximum potential work attainable when the system achieves the equilibrium with the environment, namely, its exergy (See section 3.1.2).

Thus, a further understanding on the relation between the reactor parameters and the exergy destroyed in it can be achieved by considering the combined energy and entropy balance of a non-fully reversible fuel cell and heat pump set. It can be demonstrated that the total irreversibilities in the system are given by Eq. (20):

$$B_{dest} = T_o S_{gen} = n_{N_2,inlet}\xi\left(T_o \Delta s_{reaction} - \Delta h_{reaction}\right) - \left[Q_H\left(1-\frac{T_o}{T_H}\right) - Q_L\left(1-\frac{T_o}{T_L}\right)\right] \tag{20}$$

where the term in brackets represents the exergy recovered as work after accounting for the irreversibilities present in the fuel cell and the actual heat pump. The combined efficiency of the mechanical analogy of the chemical system is calculated as:

$$\eta_{reactor} = \eta_{fuel\ cell}\ \eta_{heat\ pump} = \frac{W}{n_{N_2,inlet}\xi\left(T_o \Delta s_{reaction} - \Delta h_{reaction}\right)} \cdot \frac{Q_H\left(1-\frac{T_o}{T_H}\right) - Q_L\left(1-\frac{T_o}{T_L}\right)}{W} \tag{21}$$

The reactor conversion ξ reduces as the temperature increases [57] and its relation with the equilibrium constant K_P is given by Eq.(22):

$$K_P = \frac{a_{NH_3}}{a_{H_2}^{1.5} \cdot a_{N_2}^{0.5}} = \frac{\Theta_{NH_3} + 2\xi}{\left(1-\xi\right)^{0.5}\left(\Theta_{H_2} - 3\xi\right)^{1.5}}\left(\frac{1}{y_{N_2}^{inlet}} - 2\xi\right)\frac{\gamma_{NH_3}}{\gamma_{N_2}^{0.5} \cdot \gamma_{H_2}^{1.5}}\frac{1}{P} = f(\mathrm{T}) \tag{22}$$

where a_i is the activity of the species *i*.

Some conclusions can be withdrawn from Eqs. (20-22). First, it is important to notice that, for the adiabatic reactor, the temperatures T_H and T_L in Eq. (20) cannot vary independently since, as the inlet temperature T_L increases, the outlet temperature T_H also increases, but at expense of a decrease of the reactor conversion ξ, and thus, of the available reaction enthalpy. Additionally, as the inlet temperature T_L is reduced to the lowest allowable limit, the first term in the right hand side of Eq. (20) increases because the adiabatic reaction conversion increases, Eq. (22). But also the second term inside the brackets of Eq. (20) reduces, which makes the total exergy destroyed dependent on the highest temperature T_H attained. This temperature may vary depending on the recycle rate of inerts, ammonia and reactants, as well as on the approach to equilibrium. If the mixture is shifted away from equilibrium, i.e. if the reactor outlet temperature T_H is reduced after the first conversion bed, the

reactor conversion can be further increased in a second bed. Then, the chemical exergy available can be further exploited, but not without triggering more exergy destruction.

On the other hand, if the reactor inlet temperature T_L is increased (e.g. by preheating the reactor feed), not only the second term inside the brackets of Eq. (20) increases, but also the conversion-related term reduces, and the exergy destroyed is also reduced. Where not for the reactant preheating, the exergy recovered at high temperature would have a lower exergy value due to the reduced chemical conversion. This idea is the basis of the Counteraction principle applied to an exothermic reactor. Accordingly, there should be an intermediate optimal temperature that keeps the exergy destruction to the minimum, while guaranteeing the required reaction conversion [37]. Finally, as the reactor inlet temperature eventually approaches the reaction outlet temperature, the reactor conversion vanishes and the catalytic bed becomes a letdown system (pressure drop only). The pressure-related share of the physical exergy is degraded. Differently from Eq. (19), the pressure drop related irreversibilities can still be accounted for by using Eq. (20).
It is also noteworthy that, if the reactor pressure is increased, the activity coefficient of ammonia reduces while the respective coefficients of nitrogen and hydrogen increases, thus shifting the per-pass conversion to the product equilibrium. Pressure drop losses are generally around 5% of total reactor losses [22] and have been largely reduced so far by using different radial-axial gas flow reactor configurations [33].

Figure 8 shows the chemical exergy consumed (ΔB^{CH}) along with the exergy efficiency at which this exergy is converted into physical exergy (ΔB^{PH}). The reactor bed conversion and the autothermal heat exchanger (ATHE) performance are also represented. For the first reactor bed, the conversion in the SP200 is 29% higher than of SP150, whereas the exergy consumed and destroyed are slightly higher and lower, respectively. Higher reaction conversions are also attained for the subsequent catalyst beds of SP200, but at slightly higher exergy efficiencies. The most remarkable difference comes up from the ATHE that preheats the inlet of the first reactor bed. For SP150, the exergy destroyed in the ATHE is almost doubled due to an increase of the molar flow of the reactor feed (27%). The lower conversion and increased recycle rates of SP150 are responsible for the large associated heat transfer irreversibilities. In the case of DP configuration, both the reactor conversion and the chemical exergy consumption are reduced if compared with SP200. In this way, large driving forces are reduced while improving the exergy efficiency of the exothermic beds.

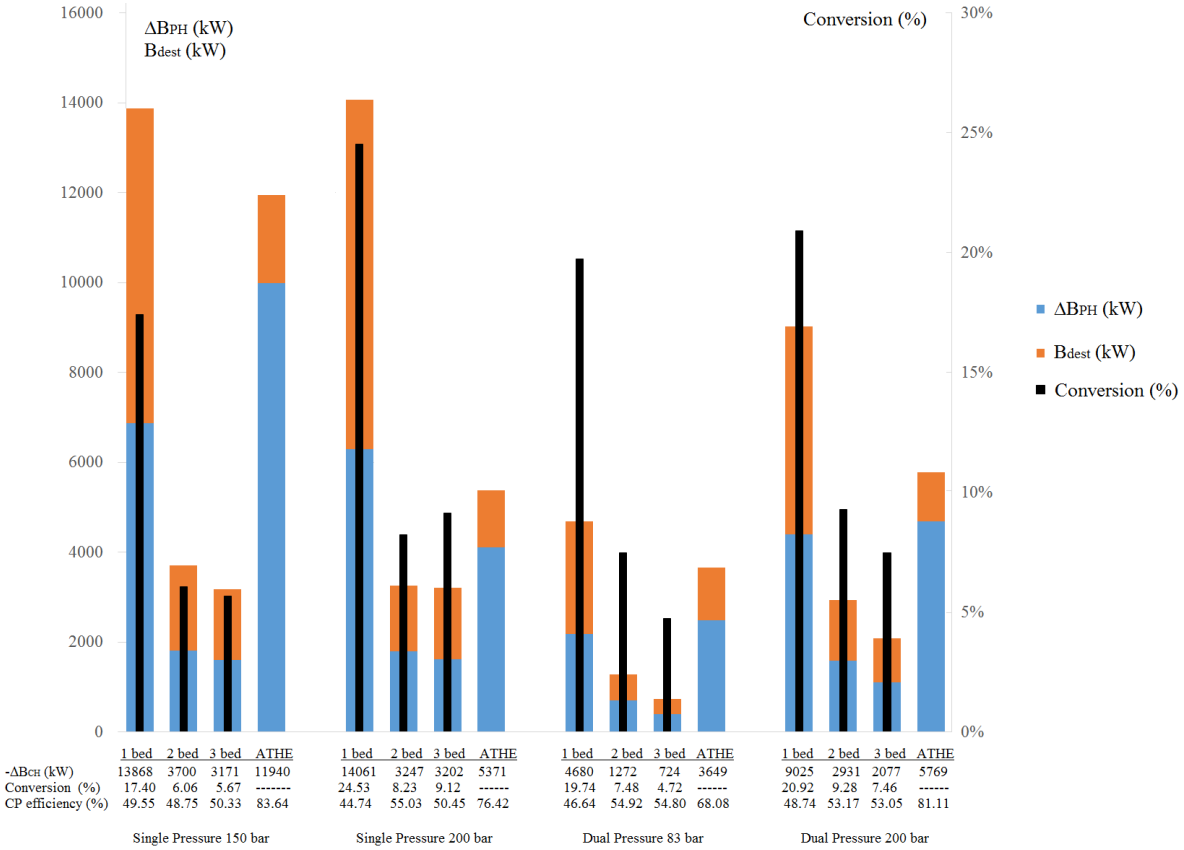

Fig. 8. Consumed-produced (CP) efficiency of the reactor beds and its relation with the reactor conversion and the auto-thermal heat exchanger (ATHE) performance.

Figure 9 and 10 present the percentage and detailed exergy destruction breakdown for representative components of the ammonia loop. The introduction of the additional once-through reactor in the DP systems increases the reaction-based irreversibilities about 1.4 and 4.2%, if compared with SP150 and SP200 configurations, respectively. However, the total (plant-wide) exergy destruction of the former is much lower (3.7 and up to 15%, respectively). In fact, the effect of introducing an additional irreversibility source is offset by a more uniform distribution of the irreversibilities in the whole loop. This is in agreement with the Counteraction principle applied to reducing-volume reactions. The incremental pressures reduce the power consumption by lowering the makeup syngas compression and the refrigeration duties (e.g., avoidable losses) while more efficient conversions are carried out at lower pressures.

In order to achieve higher ammonia yields, the conversion is often intentionally reduced in the industrial practice by increasing the circulation rate. This practice requires more exergy to overcome increased pressure drops, increasing so the avoidable exergy losses [74]. Alternatively, better conversions at lower pressures and higher overall reactor efficiencies could be obtained if a set of low ignition temperature catalysts were developed and suitably distributed along the reactor beds. In this way, improved conversion rates at different bed temperatures and compositions could be obtained [11, 25, 34]. It would also be desirable to perform the reaction under *resisted conditions* [62], so that the chemical exergy can be maximally exploited. Unfortunately, this is a practical shortcoming in large-scale industrial applications, because it would require slow enough, quasi-reversible conditions [80] or strict coupling between thermal and chemical forces of the system which is not always feasible [83].

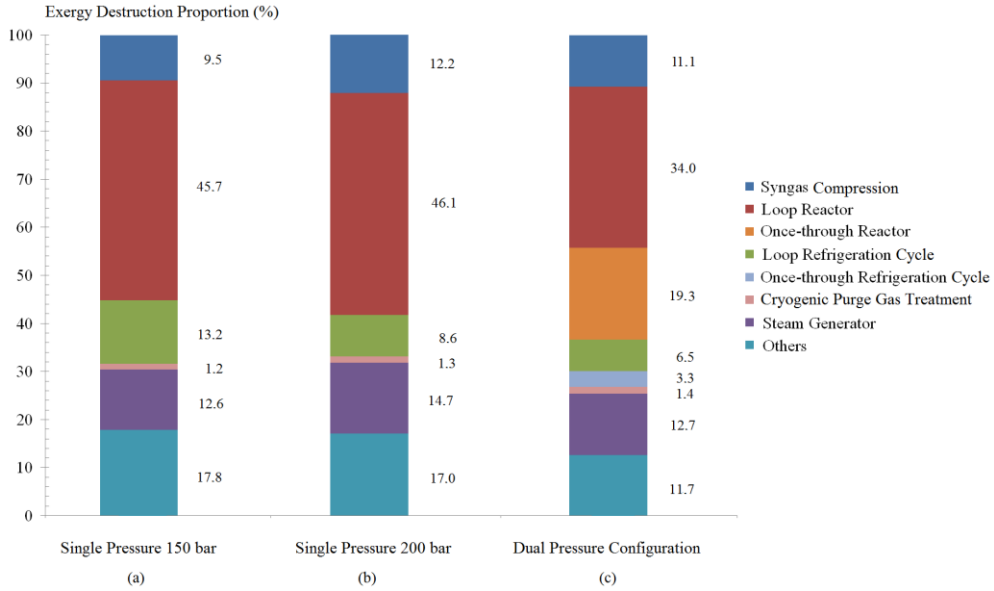

Fig. 9. Exergy destruction breakdown for representative components of the ammonia loop: (a) single pressure 150 bar, (b) single pressure 200 bar, (c) dual pressure configuration.

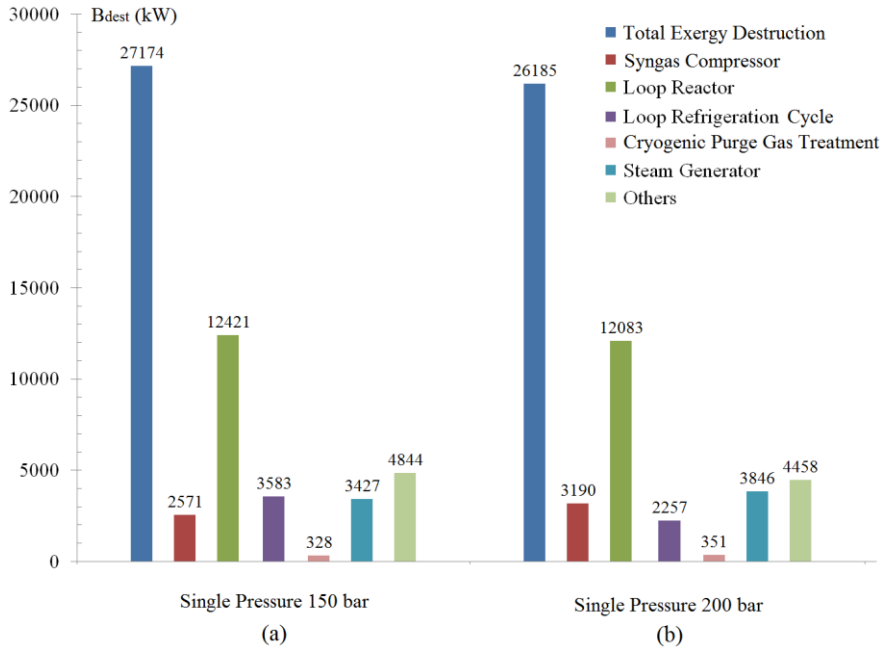

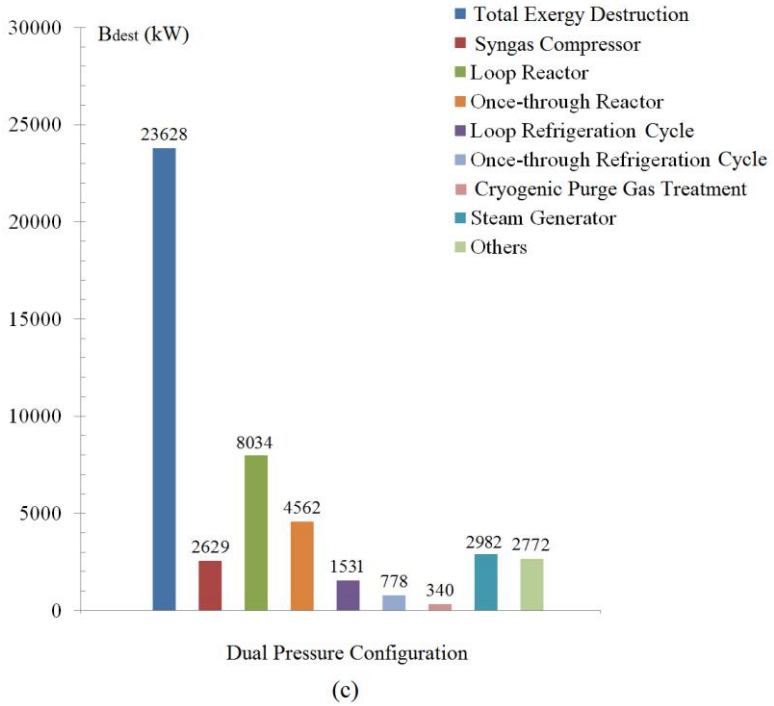

Fig. 10. Exergy destruction of representative components of the ammonia loop: (a) single pressure 150 bar, (b) single pressure 200 bar, (c) dual pressure configuration.

4.4. Combined exergy and heat integration analysis

When considering a series of adiabatic catalytic beds with intercooling, the reduction of the exergy destruction becomes a problem of determining the best alternative to recover as much as the physical exergy of the reactor effluent by producing, e.g. high pressure steam. However, depending on the steam network design (e.g. pressure and superheating in the headers, water flow rate, heat transfer rate, minimum temperature difference, etc.), the irreversibilities owed to the large driving forces in the steam boiler as well as the losses to the ambient through the cooling water, may increase. The fact that steam is obtained at a temperature of only 310°C and not the highest one available at the reactor outlet (>430°C) carries a certain amount of irreversibilities. This is clearly shown in Fig. 11, where the Carnot factor is plotted against the enthalpy change in the so-called hot and cold Carnot composite curves (CCC) and grand composite curves (CGCC) of the heat exchanger network. Since the area below the hot and cold Carnot composite curves represent the exergy transferred from/to the hot/cold stream, respectively, the area between the two curves stands for the irreversibilities associated to the heat transfer between the ammonia loop streams, according to Eq. (23):

$$B^{Q} = \begin{cases} \int \left(1 - \frac{T_0}{T}\right) \delta Q_T & if \quad T > T_0 \\ \int \left(\frac{T_0}{T} - 1\right) \delta Q_T & if \quad T < T_0 \end{cases} \tag{23}$$

where T is the temperature at which the heat rate, Q, is transferred. It is important to mention that the term in parenthesis in Eq. (23) does not correspond to the Carnot efficiency of the reversible Carnot cycle used to determine the potential work production from a heat source. Thus, this term can be higher than the unity indeed, indicating that at temperatures lower than 0.5 times the ambient

temperature T_o, the exergy associated to the heat transferred is higher than the heat transferred itself. This is the case of the cryogenic applications occurring in the cold box of the purge gas treatment. It is also important to point out that at temperatures below that of the ambient, the exergy is transferred from the cold to the hot stream, differently from the case in which $T>T_o$. It explains why the cold Carnot composite curves shifts to above the hot one for $T<T_o$ in Fig. 11.

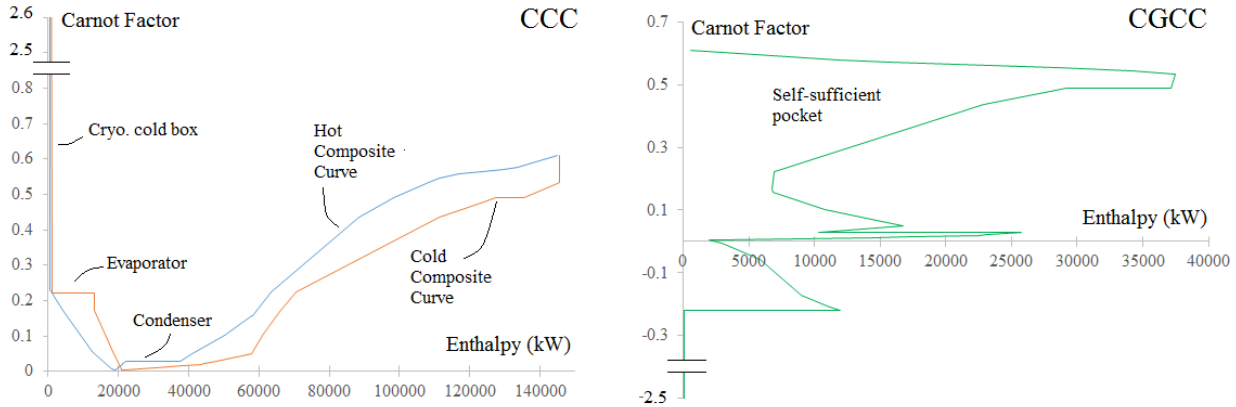

(a) Single pressure 150 bar

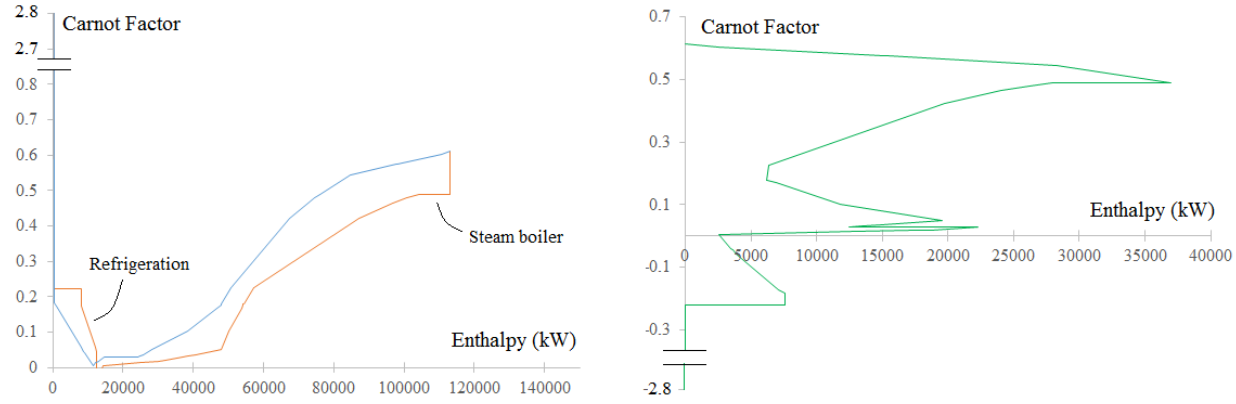

(b) Single pressure 200 bar

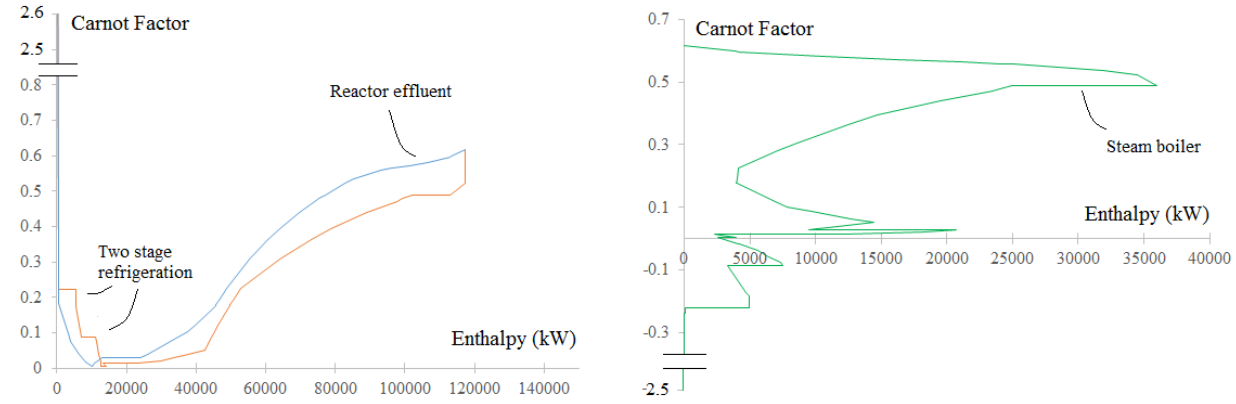

(c) Dual pressure configuration

Fig. 11. Hot and cold Carnot composite curves (CCC; left) and Carnot grand composite curves (CGCC; right) for the different ammonia loop configurations. For CCC, the Carnot factor is calculated as $(T_o/T)-1$ if $T<To$; for the sake of clarity, CGCC's Carnot factors have been mirrored for $T<T_o$.

From the CCCs in Fig. 11(a), it is striking the more extended enthalpy span in the SP150 configuration indicating larger heat transfer rates. This leads to an increased exergy destroyed in the heat exchanger network (i.e. area in between the two curves) if compared with the SP200 and dual pressure arrangements. At the level of temperature of the evaporator and condenser of the refrigeration cycle, wider plateaus generate an increased amount of irreversibilities, which can be tackled by carrying out the refrigeration process at different pressures, as in the case of the DP ammonia loop configuration (Fig. 11(c)). On the other hand, a large potential of exergy recovery can be still envisaged in all the three cases as concerns the self-sufficient area comprised to the left of the CGCC (Figs.11(a-c), right). In order to profit this potential, some authors proposed the expansion of the reactor effluent in ammonia expanders in lieu of steam boilers [30]. Although this modification would not totally render the ammonia unit self-sufficient in terms of power consumption, it is claimed that the use of an expander would profit more rationally the thermo-mechanical exergy embodied in the reactor effluent. Since the exergy of the heat is transformed directly into work, the exergy losses due to the heat transfer driving forces and those related to the steam turbine condenser could be avoided. Furthermore, despite the power consumption and specific irreversibilities are still largely dependent on the expansion pressure, the specific work required per unit of mass of product is reported as 44-75% lower compared to the conventional boiler-based system [30]. Non-conventional approaches will be worthy to explore considering the current limited room for improvement in the reactive components. In fact, the highest exergy saving potentials are expected from the reevaluation of the high temperature gas-gas heat exchangers (1500-2800kW of exergy destroyed) and the compression train [73], alongside with a reduction of the costly refrigeration. The energy-intensive nature of the current technical process is in fact mainly due to the large amount of exergy consumed in the makeup syngas compression, refrigeration and circulation systems (10.6 -14.4 MW). For instance, a benefit of the DP system is that the makeup gas is incidentally refrigerated in the way to the high pressure stage. Since the compressor operates at lower temperatures than in SP200, less exergy is consumed and destroyed. This also compensates the pressure drop throughout the additional once-through converter [32].

Finally, a large amount of the power consumed eventually ends up in the cooling water utility and rejected to the environment. However, economic and thermodynamics issues render often prohibitive any attempt to recover this exergy at low temperatures (< 360 K), as summarized in Table 5:

Table 5. Cooling duty and total exergy associated at selected heat transfer temperatures.

	SP150	**SP200**	**DP**
Cooling duty (kW)	34,120	31,639	28,373
Exergy associated at 360 K (kW)	1902	2114	1720
Exergy associated at 300 K (kW)	210	195	175
Exergy destroyed share			
Compressor intercooling (%)	42.0	51.2	46.0
Refrigeration condenser (%)	27.4	15.7	21.8
CW for first separator (%)	30.6	33.1	32.2

Thus, since these losses are not anymore recovered, they are here considered as exergy destroyed. As a final remark, it is pointed out that the intercooling system of the multistage syngas compressor accounts for 790-1082 kW out of 1700-2100 kW of the exergy destroyed through the cooling utility, as shown in Table 5 (i.e. 42-51%). This loss could only be eliminated if ammonia loops were redesigned

to operate at lower pressure and temperatures. Moreover, refrigeration is expensive and its use should be minimized favoring the use of cooling water when applicable.

4.5. Exergy performance and the role of the purge gas treatment unit

For the sake of comparison, the results of this work are compared against the overall exergy destroyed in the best case scenarios of two ammonia units operating under a single loop at 150 and 200 bar, respectively, as reported in previous studies [74]. In such studies, the valuable hydrogen contained in the purge gas is neither recovered nor recycled to the ammonia loop via a cryogenic unit. As expected, by extending the boundaries of the thermodynamic system, the overall unit irreversibilities in the present work increase about 2.2 and 2.4% for the SP150 and SP200 configuration, respectively. However, by considering the total exergy destruction rate in the DP configuration (23,628 kW), this value is found to be considerably lower than those reported for those best case scenarios without purge gas recovery, i.e. 26,537 kW at 150 bar and 25,603 kW at 200 bar, or 13.0% and 9.8% lower, respectively. This highlights the potential benefits of using a purge gas treatment unit in terms of exergy destruction reduction. It must be pointed out that nitrogen recovery is less attractive than hydrogen, since ratios of H/N < 3.0 at the front-end syngas production unit would allow transferring some of the primary reformer duty to the secondary reformer [33]. Consequently, the current bottlenecks on large capacity reformers used for hydrogen production in ammonia plants such MEGAMMONIA ® can be partly overcome [35].

5. Conclusions

In this papers, the exergy analysis is used to show the application of the Counteraction principle for reducing the exergy destruction rates arisen from the higher conversions per pass in ammonia synthesis. Exergy efficiency indicators suitability was discussed in terms of sensibility and ammonia unit scope. By using a once-through reactor operating at lower pressures, it been shown the possibility to offset the exergy losses due to the additional pressure drop and also increase the amount of waste heat recovered via a more efficient recovery of the enthalpy of reaction. As a result, the introduction of a dual pressure process increases the overall exergy performance of the ammonia unit in more than 10.13% while reduces the circulation rates, which in turn reduces the exergy consumption in the condensation and refrigeration systems, the size and the economic costs. Exergy also provides a better insight into the reaction driving forces at variable temperatures and pressures, which allows proposing mitigation tasks that take the irreversibilities down. However, other non-conventional approaches are still worthy to be explored, considering the current limited room for improvement in the reactive components. Among the highest exergy saving potentials are the reevaluation of the high temperature gas-gas heat exchangers and the compression train and refrigeration power consumption. The challenge is thus to keep the rate of reaction at acceptable levels whereas the effective driving forces are lowered and the net power input to the plant is reduced. Further decision-making criteria are required in order to prioritize the objective of the ammonia production unit in terms of higher ammonia yields (Le Chatelier principle) or exergy destruction minimization. In any case, both objectives rely on principles based on Laws of Thermodynamics, and, as such, they can be used to reduce the consumption of the resources, while decreasing the environmental impact. Other decision-making criteria, such as market-driven or geographic-based criteria, are out of the scope of this study.

Acknowledgments

The first author would like to acknowledge the National Agency of Petroleum, Gas and Biofuels – ANP and its Human Resources Program (PRH/ANP Grant 48610.008928.99), and the Administrative

Department of Science, Technology and Innovation – COLCIENCIAS for supporting the first stage of this work. He also would like to knowledge the Swiss Government Excellence Scholarship program (2016.0876) and the Ecole Polytechnique Federal de Lausanne for supporting the second stage of this study. Second author would like to thank National Research Council for Scientific and Technological Development, CNPq (grant 306033/2012-7).

Appendix

Table A.1-A.3 summarizes some thermodynamic properties of the process streams, according to Figs. 1 and 2.

Table A.1. Selected process data of the ammonia synthesis unit operating at 150 bar (1000 metric tons of NH_3 per day).

Nº	Stream	n (kmol/h)	T (°C)	P (bar)	B^{CH} (kW)	B^{PH} (kW)	N_2 (%)	H_2 (%)	NH_3 (%)	CH_4 (%)	Ar (%)
1	Makeup syngas	5282.0	35.1	34.7	265469	12927	25.0	73.6	0.0	1.0	0.4[1]
2	W compr. total	--	--	--	--	8193	--	--	--	--	--
3	Fresh syngas	5362	35.9	150.8	270836	18825	24.8	74.0	0.0	1.0	0.2
4	To 2° separator	22660	-20.0	147.2	1477609	80025	20.9	59.6	9.4	7.9	2.2
5	W loop refrig	--	--	--	--	4890	--	--	--	--	--
6	Recycled syngas	20979	22.4	147.2	1326707	73057	22.5	64.4	2.2	8.5	2.4
7	W circulator	--	--	--	--	498	--	--	--	--	--
8	To ATHE	20979	254.2	150.8	1326707	84026	22.5	64.4	2.2	8.5	2.4
9	Bed 1 feed	20979	365.0	150.8	1326707	94013	22.5	64.4	2.2	8.5	2.4
10	Bed 1 outlet	19335	494.6	149.7	1312839	100885	20.2	57.1	10.9	9.2	2.6
11	Bed 2 feed	19335	384.7	149.7	1312839	88945	20.2	57.1	10.9	9.2	2.6
12	Bed 2 outlet	18861	422.9	148.6	1309138	90748	19.4	54.8	13.7	9.4	2.7
13	Bed 3 feed	18861	400.0	148.6	1309138	88367	19.4	54.8	13.7	9.4	2.7
14	Bed 3 outlet	18446	433.8	147.2	1305968	89963	18.8	52.7	16.2	9.6	2.7
15	BFW inlet	3997	110.1	100.0	999	1124	--	--	--	--	--
16	Steam[2] outlet	3997	310.0	100.0	999	12909	--	--	--	--	--
17	To gas-gas HE	18446	300.0	147.2	1305968	77133	18.8	52.7	16.2	9.6	2.7
18	Purge gas	284	30.0	147.2	19838	982	19.6	55.2	12.3	10.0	2.9
19	NH_3 Product	2544	-2.6	147.2	233816	4456	0.2	0.4	98.3	1.1	0.0
20	Flashed NH_3	8	8.6	80.0	756	14	0.2	0.2	98.8	0.8	0.0
21	Aquammonia[3]	162	75.9	80.0	2415	23	--	--	16.6	--	--
22	Purge to refrig.	249	10.0	79.6	16722	757	22.4	62.9	0.0	11.4	3.3
23	W cryo refrig	--	--	--	--	36	--	--	--	--	--
24	To cold box	249	-30.0	79.6	16722	769	22.4	62.9	0.0	11.4	3.3
25	To cryo sep	249	-190.0	79.6	16722	1328	22.4	62.9	0.0	11.4	3.3
26	Expanded liquid	89	-197.1	1.0	6899	478	52.0	7.7	0.0	31.8	8.5
27	HP H_2-N_2 mixture	87	87	232.0	5344	338	6.1	93.3	0.0	0.2	0.4
28	W expander	--	--	--	--	89	--	--	--	--	--
29	LP H_2-N_2 mixture	74	30.0	80	5344	225	6.1	93.3	0.0	0.2	0.4
30	Fuel Gas	89	-26.7	1.0	6899	3	52.0	7.7	0.0	31.8	8.5

1. Included 0.2% water; 2. Vapor fraction 0.29; 3. Aqueous solution 83.4% water.

Table A.2. Selected process data of the ammonia synthesis unit operating at 200 bar (1000 metric tons of NH_3 per day).

Nº	Stream	n (kmol/h)	T (°C)	P (bar)	B^{CH} (kW)	B^{PH} (kW)	N_2 (%)	H_2 (%)	NH_3 (%)	CH_4 (%)	Ar (%)
1	Makeup syngas	5282	35.1	34.7	264574	12927	25.2	73.4	0.0	1.0	0.4[1]
2	W compr. Total	--	--	--	--	9954	--	--	--	--	--
3	Fresh syngas	5421	36.2	200.0	273712	20206	24.7	74.1	0.0	1.0	0.2
4	To 2° separator	16206	-20	198.7	982612	60927	21.1	65.2	6.5	5.5	1.7
5	W loop refrig	--	--	--	--	3090	--	--	--	--	--
6	Recycled syngas	15412	11.6	198.7	911877	57281	22.2	68.5	1.8	5.7	1.8
7	W circulator	--	--	--	--	101	--	--	--	--	--
8	To ATHE	15412	241.9	200.0	911877	64309	22.2	68.5	1.8	5.7	1.8
9	Bed 1 feed	15412	310.0	200.0	911877	68414	22.2	68.5	1.8	5.7	1.8
10	Bed 1 outlet	13731	496.9	199.6	897816	74705	18.8	58.6	14.3	6.3	2.0
11	Bed 2 feed	13731	429.3	199.6	897816	69333	18.8	58.6	14.3	6.3	2.0
12	Bed 2 outlet	13305	477.7	199.2	894570	71120	17.8	55.7	17.9	6.6	2.0
13	Bed 3 feed	13305	380.0	199.2	894570	63748	17.8	55.7	17.9	6.6	2.0
14	Bed 3 outlet	12873	430.0	198.7	891367	65364	16.8	52.4	21.9	6.8	2.0
15	BFW inlet	3997	110.1	100.0	999	1124	--	--	--	--	--
16	Steam[2] outlet	3997	310.0	100.0	999	13466	--	--	--	--	--
17	To gas-gas HE	12873	300.0	198.7	891367	56547	16.8	52.4	21.9	6.8	2.0
18	Purge gas	312	30.0	198.7	20527	1151	19.4	60.7	9.8	7.7	2.4
19	NH_3 Product	2570	15.0	198.7	235915	4637	0.4	0.7	97.7	1.2	0.0
20	Flashed NH_3	11.5	-2.6	80.0	1057	19.2	0.1	0.2	99.1	0.6	0.0
21	Aquammonia[3]	118.9	52.5	80.0	1739	10	0.0	0.0	16.2	0.0	0.0
22	Purge to refrig.	281.5	10.0	79.6	17786	855.6	21.5	67.3	0.0	8.5	2.7
23	W cryo. refrig	--	--	--	--	40	--	--	--	--	--
24	To cold box	282	-30.0	79.6	17787	869	21.45	67.3	0.0	8.5	2.7
25	To cryo. Sep	282	-195.0	79.6	17786	1527	21.45	67.3	0.0	8.5	2.7
26	Expanded liquid	89	-199.1	1.0	5867	500	57.6	7.7	0.0	26.6	8.1
27	HP H_2-N_2 mixture	146	83.2	225.1	9121	564	4.8	94.9	0.0	0.1	0.2
28	W expander	--	--	--	--	144	--	--	--	--	--
29	LP H_2-N_2 mixture	46	34.0	79.6	2880	140	4.8	94.9	0.0	0.1	0.2
30	Fuel Gas	89	12.5	1.0	5867	0.1	57.6	7.7	0.0	26.6	8.1

1. Included 0.2% water; 2. Vapor fraction 0.34; 3. Aqueous solution 83.8% water.

Table A.3. Selected process data of the ammonia synthesis unit operating at dual pressure 83/200 bar (1000 metric tons of NH_3 per day).

Nº	Stream	n (kmol/h)	T (°C)	P (bar)	B^{CH} (kW)	B^{PH} (kW)	N_2 (%)	H_2 (%)	NH_3 (%)	CH_4 (%)	Ar (%)
1	Makeup syngas	5282	35.1	34.7	264574	12927	25.2	73.4	0.0	1.0	0.4[1]
2	W compr. Total	--	--	--	--	8516	--	--	--	--	--
3	OTR feed preheat	5276	35.0	83.2	264598	16209	25.3	73.5	0.0	1.0	0.2
4	OTR Bed 1 feed	5276	290.0	83.2	264598	19455	25.3	73.5	0.0	1.0	0.2
5	OTR Bed 1 outlet	4751	466.9	83.1	259918	21638	22.5	65.0	11.1	1.2	0.2
6	OTR Bed 2 feed	4751	370.0	83.1	259918	19285	22.5	65.0	11.1	1.2	0.2
7	OTR Bed 2 outlet	4591	425.6	83.0	258647	19984	21.5	62.1	15.0	1.2	0.2
8	OTR Bed 3 feed	4591	370.0	83.0	258647	18687	21.5	62.1	15.0	1.2	0.2
9	OTR Bed 3 outlet	4497	402.9	82.9	257923	19084	20.9	60.2	17.4	1.3	0.2
10	To OTR refrig	4497	46.0	82.9	257923	13708	20.9	60.2	17.4	1.3	0.2
11	W refrig OTR	--	--	--	--	827	--	--	--	--	--
12	OTR NH_3 product	474	5.0	82.9	42559	752	0.1	0.2	98.6	0.1	0.0
13	To loop Syngas	4023	5	82.9	216033	12338	23.4	67.3	7.8	1.3	0.2
14	Fresh syngas	4170	36.1	199.3	197090	15477	22.8	68.2	7.5	1.3	0.2

Nº	Stream	n (kmol/h)	T (°C)	P (bar)	B^{CH} (kW)	B^{PH} (kW)	N_2 (%)	H_2 (%)	NH_3 (%)	CH_4 (%)	Ar (%)
15	To 2° separator	8467	-20.0	199.3	562287	31737	19.9	59.1	10.0	8.3	2.7
16	W loop refrig	--	--	--	--	2022	--	--	--	--	--
17	Recycled syngas	7763	19.2	199.3	498763	28819	21.7	64.5	1.9	9.0	2.9
18	W circulator	--	--	--	--	42.9	--	--	--	--	--
19	To ATHE	11933	257.2	200.0	723500	50466	22.1	65.7	3.9	6.3	2.0
20	Bed 1 feed	11933	350.0	200.0	723500	55145	22.1	65.7	3.9	6.3	2.0
21	Bed 1 outlet	10831	505.0	199.8	714475	59545	19.2	57.2	14.5	6.9	2.2
22	Bed 2 feed	10831	413.0	199.8	714475	53775	19.2	57.2	14.5	6.9	2.2
23	Bed 2 outlet	10444	468.6	199.6	711544	55363	18.1	53.8	18.7	7.2	2.2
24	Bed 3 feed	10444	400	199.6	711544	51227	18.1	53.8	18.7	7.2	2.2
25	Bed 3 outlet	10162	441.1	199.3	709467	52329	17.2	51.1	22.0	7.4	2.3
26	BFW inlet	3997	110.1	100.0	999	1124	--	--	--	--	--
27	Steam[2] outlet	3997	310.0	100.0	999	14426	--	--	--	--	--
28	To gas-gas HE	10162	300.0	199.3	709467	44668	17.2	51.1	22.0	7.4	2.3
29	Purge gas	292	30.0	199.3	19384	1076	19.9	59.1	10.0	8.3	2.7
30	NH_3 Product	2107	13.8	199.3	194283	3831	0.3	0.7	97.5	1.4	0.1
31	Flashed NH_3	11	-2.6	80.0	1010	18	0.1	0.2	99.1	0.7	0.0
32	Aquammonia[3]	118	53.2	80.0	1638	10	0.0	0.0	15.4	0.0	0.0
33	Purge to refrig.	263	10.0	79.5	16789	799	22.1	65.6	0.0	9.3	3.0
34	W cryo. refrig	--	--	--	--	40	--	--	--	--	--
35	To cold box	263	-30	79.5	16789	811	22.1	65.6	0.0	9.3	3.0
36	To cryo sep	263	-190	79.5	16789	1384	22.1	65.6	0.0	9.3	3.0
37	Expanded liquid	85	-198	1.0	5953	457	55.1	8.2	0.0	28.3	8.4
38	HP H_2-N_2 mixture	146	73.2	215.0	8954	556	6.3	93.1	0.0	0.2	0.4
39	W expander	--	--	--	--		--	--	--	--	--
40	LP H_2-N_2 mixture	32.0	33.0	79.5	1965	97.3	6.3	93.1	0.0	0.2	0.4
41	Fuel Gas	85	19.4	1.0	5953	0.1	55.1	8.2	0.0	28.3	8.4

1. Included 0.2% water; 2. Vapor fraction 0.41; 3. Aqueous solution 84.6% water.

Nomenclature

Latin Symbols

n	Nitrogen molar flow	kmol h^{-1}
a	Activity coefficient	--
B	Exergy rate	kW
BFW	Boiler feedwater	--
b^{CH}	Standard chemical exergy	kJ $kmol^{-1}$
Q	Heat transfer rate	kW
W	Power	kW
G	Superficial mass velocity of reactants	kg s^{-1} m^{-2}
Cp	Specific heat capacity	kJ $kmol^{-1}$ K^{-1}
H	Enthalpy	kW, kJ
S	Entropy	kW, kJ
Ea	Activation energy	kJ $kmol^{-1}$
r	Rate of nitrogen reaction	kmol $m^{-3}_{cat}h^{-1}$
V	Reactor volume	m^3
K_P^2	Equilibrium constant	--

k_f	Forward reaction constant	--
k_b	Backward reaction constant	--
f	Mixture component fugacity	atm
f°	Pure component fugacity	atm
x_i	Species mol fraction in liquid phase	--
y_i	Species mol fraction in vapor phase	--
P	Total reactor pressure	bar
z	Reactor length	m
D_p	Catalyst diameter	m
S_{gen}	Entropy generation rate	kJ K^{-1} h^{-1}
T	Temperature	°C, K
T_R	Reference temperature	°C, K
T_o	Ambient temperature	°C, K
ΔH_R°	Reaction enthalpy	kJ $kmol^{-1}$
ΔG	Gibbs energy reaction difference	kJ $kmol^{-1}$
Ru	Ideal gas constant	kJ $kmol^{-1}$ K^{-1}

Greek Symbols

ξ	Reactor conversion	--
μ	Dynamic viscosity	kg s^{-1} m^{-1}
ρ	Gas density	kg m^{-3}
γ_i	Species activity coefficient	--
α	Temkin-Phyzev's exponent	--
ϕ	Void fraction	--
Θ_i	Molar flow ratio *i* to nitrogen at the reactor inlet	--
ϕ'_i	Fugacity coefficient of species *i*	--
σ	Volumetric entropy generation rate	kJ $kmol^{-1}$ K^{-1} m^{-3} h^{-1}
η	Efficiency	--

Superscript and subscript

PH	Physical exergy
CH	Chemical exergy
CP	Consumed-produced efficiency
o	Ambient conditions
R	Reference conditions
M	Mass-associated exergy
Q	Heat-associated exergy
Dest	Destroyed
H	High level temperature
L	Low level temperature

References

1.Heffer, P., Prud'homme, M. *Fertilizer Outlook 2014-2018*. in *82nd IFA Annual Conference, International Fertilizer Industry Association (IFA), 26-28 May 2014*. Sydney, Australia.

2.Bhat, M., English, B.,Turhollow, A., Nyangito, H., *Energy in Synthetic Fertilizers and Pesticides: Revisited*, Department of Agricultural Ekonoplics and Rural Sociology, 1994, Oak Ridge National Laboratory: Tennessee, USA.

3.IPCC, *Reference Document on Best Available Techniques for the Manufacture of Large Volume Inorganic Chemicals - Ammonia, Acids and Fertilisers Industries*. 2007, Integrated Pollution Prevention and Control
4.Kool, A., Blonk, H., *LCI data for the calculation tool Feedprint for greenhouse gas emissions of feed production and utilization: GHG Emissions of N, P and K fertilizer production*. 2012, Blonk Consultants: Netherlands.
5.Ribeiro, P.H., *Contribution to the Brazilian databank supporting the LCA of nitrogen fertilizers [In portuguese]*, in *Polytechnic School, Department of Chemical Engineering*. 2009, University of Sao Paulo: Sao Paulo.
6.Dias,V.,Fernandes,E.,*Fertilizers:A synthetic global insight.* BNDES Setorial Rio de Janeiro, set.2006(24):p.97-138.
7.PETROBRAS. *Facts and data: Understand why we invest on fertilizers [In Portuguese]*. Accessed 14-12-2016; Available from: http://www.petrobras.com.br/fatos-e-dados/entenda-por-que-investimos-em-fertilizantes.htm.
8.CIESP. *Fertilizers: Petrobras expands its scope, May 12, 2014 [In Portuguese]*. Accessed 14-05-14; Available from: http://www.ciesp.com.br/cubatao/noticias/fertilizantes-petrobras-amplia-atuacao.
9.Appl, M., *Ullmann's encyclopedia of industrial chemistry, Vol.11. Chapter 2.*, Wiley-VCH, Editor. 2012, Wiley-VCH Verlag GmbH & Co. Weinheim.
10.Kirova-Yordanova, Z., *Thermodynamic Evaluation of Energy Integration and Cogeneration in Ammonium Nitrate Production Complexes.* International Journal of Thermodynamics (IJoT), 2013. **16**(4): p. 163-171.
11.Rafiqul, I.W., C., Lehmann, B., Voss, A., *Energy efficiency improvements in ammonia production—perspectives and uncertainties.* Energy, 2005. **30**(13): p. 2487-2504.
12.Dopper, J.G., *European Roadmap for Process Intensification*. 2007, Ministry of Economic Affairs: Delft, The Netherlands. p. 53.
13.Panjeshahi, M.H., Ghasemian Langeroudi, E., Tahouni, N., *Retrofit of ammonia plant for improving energy efficiency*. Energy, 2008. **33**(1): p. 46-64.
14.Papoulias, S., Grossmann, I., *A structural optimization approach in process synthesis—II: Heat recovery networks.* Computers & Chemical Engineering, 1983. **7**(6): p. 707-721.
15.Papoulias, S., Grossmann, I., *A structural optimization approach in process synthesis—I: Utility systems.* Computers & Chemical Engineering, 1983. **7**(6): p. 695-706.
16.Papoulias, S., Grossmann, I., *A structural optimization approach in process synthesis—III: Total processing systems.* Computers & Chemical Engineering, 1983. **7**(6): p. 723-734.
17.Yee, T.F., Grossmann, I. E., Kravanja, Z., *Simultaneous optimization models for heat integration—I. Area and energy targeting and modeling of multi-stream exchangers.* Computers & Chemical Engineering, 1990. **14**(10): p. 1151-1164.
18.Yee, T.F., Grossmann, I. E., Kravanja, Z., *Simultaneous optimization models for heat integration—III. Process and heat exchanger network optimization.* Computers & Chemical Engineering, 1990. **14**(11): p. 1185-1200.
19.Yee, T.F., Grossmann, I. E., *Simultaneous optimization models for heat integration—II. Heat exchanger network synthesis.* Computers & Chemical Engineering, 1990. **14**(10): p. 1165-1184.
20.Worrell, E., Blok, K., *Energy savings in the nitrogen fertilizer industry in the Netherlands.* Energy, 1994. **19**(2): p. 195-209.
21.Rosen, M.A., *Comparative assessment of thermodynamic efficiencies and losses for natural gas-based production processes for hydrogen, ammonia and methanol.* Energy Conversion and Management, 1996. **37**(3): p. 359-367.
22.Kirova-Yordanova, Z., *Exergy analysis of industrial ammonia synthesis.* Energy, 2004. **29**(12–15): p. 2373-2384.
23.Norskov, J.K., Bligaard, T., Rossmeisl, J., Christensen, C. H., *Towards the computational design of solid catalysts.* Nat Chem, 2009. **1**(1): p. 37-46.
24.Liu, H., *Ammonia Synthesis Catalysts: Innovation and Practice*. 2013, Beijing: Chemical Industry Press, ISBN 978-981-4355-77-3.
25.UNIDO, *Fertilizer Manual: UN Industrial Development Organization*. 3rd ed, International Fertilizer Development Center. 1998, Dordrecht, Netherlands: Kluwer Academic Publishers. 616.
26.Chorkendorff, I., Niemantsverdriet, J. W., *Concepts of Modern Catalysis and Kinetics*. 2nd ed. 2007: Wiley-VCH Verlag GmbH & Co, ISBN: 978-3-527-31672-4.
27.Jacobsen, C., *Novel class of ammonia synthesis catalysts.* Chemical Communications, 2000(12): p. 1057-1058.
28.Enthaler, S., Junge, K., Beller, M., *Sustainable Metal Catalysis with Iron: From Rust to a Rising Star?* Angewandte Chemie International Edition, 2008. **47**(18): p. 3317-3321.
29.Sahafzadeh, M., Ataei, A., Tahouni, N., Panjeshahi, M., *Integration of a gas turbine with an ammonia process for improving energy efficiency.* Applied Thermal Engineering, 2013. **58**(1–2): p. 594-604.
30.Greeff, I.L., Visser, J. A., Ptasinski, K. J., Janssen, F. J. J. G., *Integration of a turbine expander with an exothermic reactor loop—Flow sheet development and application to ammonia production.* Energy, 2003. **28**(14): p. 1495-1509.
31.Lippmann, D., Larsen, P., *Uhde dual-pressure process for large-scale ammonia plants*, in *ThyssenKrupp techforum* July 2004, Thyssenkrupp Uhde GmbH, Dortmund.

32.Lippmann, D., Larsen, J., *The Uhde Dual Pressure Process – Reliability Issues and Scale Up Consideration*, in *The 47th Annual Safety in Ammonia Plants and Related Facilities Symposium,16 - September 19, 2002*: San Diego, California, USA.
33.Nielsen, A., *Ammonia: Catalysis and Manufacture*. Vol. ISBN 9783540583356. 1995: Springer.
34.Tamaru, K., *The History of the Development of Ammonia Synthesis*, in *Catalytic Ammonia Synthesis*, J.R. Jennings, Editor. 1991, Springer US. p. 1-18.
35.Maxwell, G.,*Synthetic Nitrogen Products:A Practical Guide to the Products and Processes*2004,NewYork: Springer US.
36.Mudahar, M., Hignett, T., *Energy efficiency in nitrogen fertilizer production.* Energy Agric, 1985. **4**: p. 159-177.
37.Leites, I.L., Sama, D. A., Lior, N., *The theory and practice of energy saving in the chemical industry: some methods for reducing thermodynamic irreversibility in chemical technology processes.* Energy, 2003. **28**(1): p.55-97.
38.EFMA, *Booklet No. 1 of 8: Production of Ammonia*, in *Best Available Techniques for Pollution Prevention and Control in the European Fertilizer Industry*, Editor. 2000: Brussels, Belgium.
39.Hodge, C., Popovici, N., *Pollution Control in Fertilizer Production (Environmental Science and Pollution Control Series Book 10)*. 1st. ed. 1994: CRC Press.
40.Isalski, W.H., Tomlinson, T.R., *Expansion and compression using work generated in expansion. US4312851 A*. 1982, Isalski Wieslaw H, Tomlinson Terence R.
41.Howell, J., *The Membrane Alternative: Energy Implications for Industry: Watt Committee Report Number 21*. 1990, New York, USA: CRC Press
42.Appl, M., *Ammonia: Principles and Industrial Practice*. 1999, New York: Wiley-VCH Verlag.
43.Meindersma, G.W., Kuczynski, M., *Implementing membrane technology in the process industry: problems and opportunities.* Journal of Membrane Science, 1996. **113**(2): p. 285-292.
44.Witt, J.J., Riezebos, A., . *Upgrading a 25-year-old ammonia plant resulting in lower energy consumption and higher production capacity*. in *AIChE Ammonia Safety Symposium*. 1998. Charleston, South Carolina.
45.Ostuni, R., Filippi, E., Skinner, G.F., *Hydrogen and Nitrogen Recovery from Ammonia Purge Gas. US20130039835 A1*. 2013, Ammonia Casale SA.
46. Paul, D., Yampol'skii, Y., *Polymeric Gas Separation Membranes*. 1993: CRC Press.
47.Kent, J., *Handbook of Industrial Chemistry and Biotechnology*. 12 ed. Vol. 1. 2012.
48.Mukhopadhyay, M., *Fundamentals of Cryogenic Engineering*. 2010, Delhi: PHI Learning Pvt. Ltd.
49.Péneloux, A., Rauzy, E., Fréze, R., *A consistent correction for Redlich-Kwong-Soave volumes.* Fluid Phase Equilibria, 1982. **8**(1): p. 7-23.
50.ASPENTECH, *Aspen Physical Property System - Physical Property Methods V7.3 - User Guide*. 2011.
51.ASPENTECH, *Aspen Plus - Aspen Plus Ammonia Model*. 2008.
52.Abdollahi-Demneh, F., Moosavian, M., Omidkhah, M., Bahmanyar, H., *Calculating exergy in flowsheeting simulators: A HYSYS implementation.* Energy, 2011. **36**(8): p. 5320-5327.
53.Turton, R.B., R. Whiting, W., Shaeiwitz, J., *Analysis, Synhtesis and Design of Chemical Processes*. 3rd ed. 2009, New York: Prentice Hall.
54.Dyson, D.C., Simon, J. M., *Kinetic Expression with Diffusion Correction for Ammonia Synthesis on Industrial Catalyst.* Industrial & Engineering Chemistry Fundamentals, 1968. **7**(4): p. 605-610.
55.Singh, C.P., Saraf, D. N., *Simulation of Ammonia Synthesis Reactors.* Industrial & Engineering Chemistry Process Design and Development, 1979. **18**(3): p. 364-370.
56.Fogler, S.H., *Elements of Chemical Reaction Engineering*. 4th Edition ed. 1986: Prentice-Hall.
57.Gillespie, L., Beattie, J. A., *The Thermodynamic Treatment of Chemical Equilibria in Systems Composed of Real Gases. I. An Approximate Equation for the Mass Action Function Applied to the Existing Data on the Haber Equilibrium.* Physical Review, 1930. **36**(4): p. 743-753.
58.Imperial Chemical Industries, *Catalyst handbook: With special reference to unit processes in ammonia and hydrogen manufacture*. 1970: Wolfe Publishers.
59.Sandler, S., Orbey, H., *Modeling Vapor-Liquid Equilibria: Cubic Equations of State and Their Mixing Rules*, ed. C.U. Press. 1998: Cambridge Series on Chemical Engineering.
60.Szargut, J., Morris, D, Steward, F, *Exergy analysis of thermal, chemical, and metallurgical processes*. 1988, New York: Hemisphere Publishing Corporation.
61.Ayres, R., Warr, B., *Accounting for growth: the role of physical work.* Structural Change and Economic Dynamics, 2005. **16**(2): p. 181-209.
62.Denbigh, K.G., *The second-law efficiency of chemical processes.* Chemical Engineering Science, 1956.**6**(1):p.1-9.
63.Kjelstrup, S., Bedeaux, D., Johannessen, E., Gross, J., *Non-Equilibirum Thermodynamics for Engineers*. 2010, Trondheim: World Scientific Publishing.

64.Johannessen, E., Kjelstrup, S., *Minimum entropy production rate in plug flow reactors: An optimal control problem solved for SO2 oxidation.* Energy, 2004. **29**(12–15): p. 2403-2423.
65.Marmolejo-Correa, D., Gundersen, T., *A comparison of exergy efficiency definitions with focus on low temperature processes.* Energy, 2012. **44**(1): p. 477-489.
66.Tsatsaronis, G., *Thermoeconomic analysis and optimization of energy systems.* Progress in Energy and Combustion Science, 1993. **19**(3): p. 227-257.
67.Brodyansky, V.M., Sorin, M.V. and Le Goff, P., *The Efficiency of Industrial Processes: Exergy Analysis and Optimization*. 1994, Amsterdam: Elsevier.
68.Sorin, M., Lambert, J., Paris, J., *Exergy Flows Analysis in Chemical Reactors.* Chemical Engineering Research and Design, 1998. **76**(3): p. 389-395.
69.Szargut, J., *Exergy in thermal systems analysis*, in *Thermodynamic optimization of complex energy systems, NATO Science Series 69*, A. Bejan, Mamut, E., Editors. 1999, Springer.
70.Flórez-Orrego, D., Oliveira Junior, S., *On the efficiency, exergy costs and CO2 emission cost allocation for an integrated syngas and ammonia production plant.* Energy, 2016. **117, Part 2**: p. 341-360.
71.Denbigh, K.G., *The Principles of Chemical Equilibrium: With Applications in Chemistry and Chemical Engineering* 1981: Cambridge University Press.
72.Tock, L., Maréchal, F., Perrenoud, M., *Thermo-environomic evaluation of the ammonia production.* The Canadian Journal of Chemical Engineering, 2015. **93**(2): p. 356-362.
73.Penkuhn, M., Tsatsaronis, G., *Comparison of different ammonia synthesis loop configurations with the aid of advanced exergy analysis*, in *29th International Conference on Efficiency, Cost, Optimization, Simulation and Environmental Impact of Energy Systems, ECOS 2016*. 2016: Portoroz, Slovenia.
74.Flórez-Orrego, D., Oliveira Jr, S., *Exergy Modeling and Optimization of an Ammonia Production Plant*, in *29th International Conference on Efficiency, Cost, Optimization, Simulation and Environmental Impact of Energy Systems, ECOS 2016*. 2016: Portoroz, Slovenia.
75.Araújo, A., Skogestad, S., *Control structure design for the ammonia synthesis process.* Computers & Chemical Engineering, 2008. **32**(12): p. 2920-2932.
76.Murase, A., Roberts, H., Converse, A., *Optimal Thermal Design of an Autothermal Ammonia Synthesis Reactor*. Industrial & Engineering Chemistry Process Design and Development, 1970. **9**(4).
77.Luyben, W., *Chapter 13 - Design and Control of a Cooled Ammonia Reactor*, in *Plantwide Control: Recent Developments and Applications*, G. Rangaiah, ariwala, V., Editor. 2012, John Wiley & Sons. p. 273-292.
78.Sorin, M., Paris, J., *Integrated exergy load distribution method and pinch analysis.* Computers & Chemical Engineering, 1999. **23**(4–5): p. 497-507.
79.Silva, J.A.M., Flórez-Orrego, D., Oliveira Jr, S., *An exergy based approach to determine production cost and CO2 allocation for petroleum derived fuels.* Energy, 2014. **67**(0): p. 490-495.
80.Hinderink, A.P., Kerkhof, F. P. J. M., Lie, A. B. K., De Swaan Arons, J., Van Der Kooi, H. J., *Exergy analysis with a flowsheeting simulator—II. Application; synthesis gas production from natural gas.* Chemical Engineering Science, 1996. **51**(20): p. 4701-4715.
81.Glavič, P., Kravanja, Z., Homšak, M., *Heat integration of reactors—I. Criteria for the placement of reactors into process flowsheet.* Chemical Engineering Science, 1988. **43**(3): p. 593-608.
82.Kotas, T., *The exergy method of thermal planta analysis*. 2 ed. 1995, Malabar, Florida: Krieger Publishing Company.
83.Kjelstrup, S., Swaan A., *Denbigh revisited: Reducing lost work in chemical processes.* Chemical Engineering Science, 1995. **50**(10): p. 1551-1560.